

This is the peer reviewed version of the following article:

Pinpointing sources of pollution using citizen science and hyperlocal low-cost mobile source apportionment / Bousiotis, Dimitrios; Damayanti, Seny; Baruah, Arunik; Bigi, Alessandro; Beddows, David C. S.; Harrison, Roy M.; Pope, Francis D.. - In: ENVIRONMENT INTERNATIONAL. - ISSN 0160-4120. - 193:(2024), pp. 1-40. [10.1016/j.envint.2024.109069]

Terms of use:

The terms and conditions for the reuse of this version of the manuscript are specified in the publishing policy. For all terms of use and more information see the publisher's website.

05/05/2026 16:43

(Article begins on next page)

Journal Pre-proofs

Full length article

Pinpointing sources of pollution using citizen science and hyperlocal low-cost mobile source apportionment

Dimitrios Bousiotis, Seny Damayanti, Arunik Baruah, Alessandro Bigi, David C.S. Beddows, Roy M. Harrison, Francis D. Pope

PII: S0160-4120(24)00655-X
DOI: <https://doi.org/10.1016/j.envint.2024.109069>
Reference: EI 109069

To appear in: *Environment International*

Received Date: 23 July 2024
Revised Date: 18 September 2024
Accepted Date: 9 October 2024



Please cite this article as: D. Bousiotis, S. Damayanti, A. Baruah, A. Bigi, D.C.S. Beddows, R.M. Harrison, F.D. Pope, Pinpointing sources of pollution using citizen science and hyperlocal low-cost mobile source apportionment, *Environment International* (2024), doi: <https://doi.org/10.1016/j.envint.2024.109069>

This is a PDF file of an article that has undergone enhancements after acceptance, such as the addition of a cover page and metadata, and formatting for readability, but it is not yet the definitive version of record. This version will undergo additional copyediting, typesetting and review before it is published in its final form, but we are providing this version to give early visibility of the article. Please note that, during the production process, errors may be discovered which could affect the content, and all legal disclaimers that apply to the journal pertain.

© 2024 Published by Elsevier Ltd.

Pinpointing sources of pollution using citizen science and hyperlocal low-cost mobile source apportionment

Dimitrios Bousiotis^{1*}, Seny Damayanti¹, Arunik Baruah^{2,3}, Alessandro Bigi², David C.S. Beddows¹, Roy M. Harrison^{1†} and Francis D. Pope^{1*}

¹ School of Geography, Earth and Environmental Sciences, University of Birmingham, Edgbaston, Birmingham B15 2TT, UK.

² Department of Engineering "Enzo Ferrari", University of Modena and Reggio Emilia, Modena, 41125, Italy.

³ University School of Advanced Studies IUSS Pavia, Palazzo Del Brotello, Pavia, 27100, Italy.

[†] Also at: Dept of Environmental Sciences, King Abdulaziz University, PO Box 80203, Jeddah, Saudi Arabia.

*Corresponding authors: d.bousiotis@bham.ac.uk; f.pope@bham.ac.uk

ABSTRACT

Currently, methodologies for the identification and apportionment of air pollution sources are not widely applied due to their high cost. We present a new approach, combining mobile measurements from multiple sensors collected from the daily walks of citizen scientists, in a high population density area of Birmingham, UK. The methodology successfully pinpoints the different sources affecting the local air quality in the area using only a handful of measurements. It was found that regional sources of pollution were mostly responsible for the PM_{2.5} and PM₁ concentrations. In contrast, PM₁₀ was mostly associated with local sources. The total particle number and the lung deposited surface area of PM were almost solely associated with traffic, while black carbon was associated with both the sources from the urban background and local traffic. Our analysis showed that while the effect of the hyperlocal sources, such as emissions from construction works or traffic, do not exceed the distance of a couple of hundred meters, they can influence the health of thousands of people in densely populated areas. Thus, using this novel approach we illustrate the limitations of the present measurement network paradigm and offer an alternative and versatile approach to understanding the hyperlocal factors that affect urban air quality. Mobile monitoring by citizen scientists is shown to have huge potential to

enhance spatiotemporal resolution of air quality data without the need of extensive and expensive campaigns.

1. INTRODUCTION

Air pollution is a major health issue which impacts public health and the economy (Birnbaum et al., 2020; Liu et al., 2019; Rivas et al., 2021). Globally, exposure to air pollution is considered a leading risk life expectancy reduction (Forouzanfar et al., 2015), and is the leading environmental risk factor. It is estimated that approximately 9 million premature deaths per year are caused by poor air quality (Fuller et al., 2022). The dominant air pollutant with respect to human health is particulate matter (PM). Thus, actions to improve air quality, and in particular PM levels, are required. The most recent PM guidelines set by the World Health Organization (WHO) highlight that exposure to even relatively minor PM concentrations can impact upon health (World Health Organisation, 2021).

To build successful strategies for air pollution control, not only do air pollutant concentrations need to be measured, an understanding of where the air pollution comes from is also required, i.e. the sources of air pollution need to be identified and apportioned. Hence, source apportionment studies are crucially important, as these provide the link between activities and the air pollution that they create (Belis et al., n.d.; Coelho et al., 2023). To date, there have been many source apportionment studies in the scientific literature (Beddows et al., 2015; Cesari et al., 2016; Rivas et al., 2020). However, the routine application of sophisticated source apportionment techniques outside of academia is limited in many jurisdictions, leading to the use of less sophisticated methodologies for air pollution assessment. Typically, the equipment needed for source apportionment measurements are expensive and the methodologies used for their analysis are complex. As a result, source apportionment is often not part of the regulatory toolkit, even though it provides key information for air pollution management (Hopke et al., 2020; Karagulian et al., 2015).

Low-cost sensors (LCS) have caused a paradigm shift in the monitoring of air pollution allowing for pollutant mapping at a much finer spatial scale. These sensors provide air quality information at a fraction of the cost compared to research grade instruments, having both a

lower associated capital expenditure (CapEx) and operational expenditure (OpEx) (Peltier et al., 2021). Low-cost sensors are typically outperformed by the more expensive regulatory instruments (Alfano et al., 2020; Kang et al., 2022; Karagulian et al., 2019), with low-cost sensors usually lacking the accuracy, precision and sensitivity of their research grade counterparts (Austin et al., 2015; Sousan et al., 2016). The performance of sensors may degrade over time (Anastasiou et al., 2022), and need special care and calibration to provide meaningful results (Giordano et al., 2021; Hagan and Kroll, 2020; Lung, 2022; P. Wang et al., 2021). Nevertheless, their significantly lower cost and greater portability provide measurement opportunities that were not previously possible. Many studies have been conducted in which low-cost sensors have proved their potential in the field, for both outdoor and indoor applications (Ilyinskaya et al., 2017; Raysoni et al., 2023). With proper quality assurance and the correct methodologies, these sensors can provide a similar potential for a paradigm shift in source apportionment, by greatly reducing the financial burden associated with source apportionment studies. Thus, for the last 8 years, several research groups have explored the use of low-cost sensors for air pollution source apportionment (Bousiotis et al., 2023b, 2022; Westervelt et al., 2023).

Air pollution sources vary spatially and temporally, especially within urban environments (Alexeeff et al., 2018; Boogaard et al., 2011). Hence, to understand air pollution exposure, data is required at high spatial and temporal resolution. An obvious solution to this data requirement is to collect data using mobile platforms, and the use of mobile platforms for air quality measurements is not new (Seakins et al., 2002). Numerous mobile campaigns using cars, bicycles and pedestrians have been widely performed (Apparicio et al., 2021; Samad and Vogt, 2020; Singh et al., 2021; Solomon et al., 2020). The use of low-cost sensors breathe new life into such studies as they can be more versatile and widely applied (Chatzidiakou et al., 2019; deSouza et al., 2020; Macnaughton et al., 2014; S. Wang et al., 2021). Specifically, laser scattering PM sensors are considered suitable for mobile monitoring as they can record the fast temporal changes in PM concentrations (Buehler et al., 2021; Bulot et al., 2020). As a result, studies with mobile measurements can provide more detailed and spatially denser measurements, allowing for the identification of hyperlocal sources of pollution in a manner that is not possible with the existing static measurement networks (Frederickson et al., 2023; Hassani et al., 2023), even within dense network of low-cost sensors (Kumar et al., 2015).

However, to date we believe this mobile measurement approach has not been used in conjunction with source apportionment.

In the present study, mobile measurements from low-cost portable sensors were made by citizen science volunteers while on their daily walking commutes in a heavily populated residential area. The data of PM_{10} , $PM_{2.5}$ and PM_{10} from an Optical Particle Counter (OPC), equivalent black carbon (eBC) by a filter absorption photometer and total particle number (PN) along with the lung deposited surface area (LDSA) by an aerosol electrometer, all having a significantly lower cost compared to their scientific grade counterparts, were collected from walks within the study area. The PM data were analysed using Positive Matrix Factorisation (PMF), a source apportionment methodology successfully applied in previous work on datasets from both research grade instruments (Beddows et al., 2015; Harrison et al., 2011; Hopke, 2016) and low-cost sensors (Bousiotis et al., 2023b, 2022; Mills et al., 2023). While in previous studies the aim was to assess the sources of pollution affecting a greater area, in this study we present a methodology that identifies and quantifies the effect of not only the regional sources of pollution affecting the study area, but also pinpoints local point and line pollution sources within the study area. A similar task was also attempted by (Lin et al., 2023) using measurements collected by a car and ML methods, which resulted in the identification of pollution sources, rather than source apportionment which was achieved in the present study.

2. METHODS

2.1 Study area and material.

The area studied is a portion of the residential area of Selly Oak of about 1 km² (52° 26' N, 1° 55' W), 3 km SW of the city centre of Birmingham and directly south of the University of Birmingham (Figure 1). As this area is next to the University of Birmingham, it is very densely populated (about 10,000 residents in peak period) mainly with students at the University. Apart from being a residential area, in the northern and southern ends of the block are two busy roads (Bristol Road and Raddlebarn Road), as well as lots of markets and restaurants, whereas on the west side of the block lies the Selly Oak train station. The measurement period

was between the 16th and 25th of June 2023, in which ten walks with the sensor payload were made, in accordance with the ethical standards set by the University of Birmingham. Each of these walks included all the roads both in the perimeter and the inner part of the block. Four of these walks occurred in the morning (9AM to 12PM), 3 in the afternoon (12PM to 5PM) and 3 in the evening (5PM to 9PM). The sensors used for this campaign are all considered as low-cost, ranging up to a few thousands USD. The setup comprised of:

- The Alphasense OPC-N3, which is a laser scattering optical particle counter measuring in the size range between 0.35 and 40 μm , providing particle counts in 24 size bins as well as the mass concentrations for PM_{1} , $\text{PM}_{2.5}$ and PM_{10} (Alphasense, 2019a) in a 10 s resolution. A more detailed presentation of the sensor can be found in (Bousiotis et al., 2021).
- The testo DISCmini, which is a hand-held ultrafine particle counter measuring the number and average diameter of nanoparticles (10 to 700 nm) based on the electrical charge of aerosols. For the present study, the number of particles provided by this sensor will be considered as the total particle number (PN). Using the data of the particles' diameter, the DISCmini can also provide the Lung Deposited Surface Area (LDSA), a metric of the surface area concentration of the particles that deposit in the alveolar region of the human lungs. The LDSA is a very important metric as it is found to have a stronger correlation with reduced lung function and mortality than the $\text{PM}_{2.5}$ and the PM_{10} (Hennig et al., 2018; Patel et al., 2018) and can be used to provide further information about the particles' characteristics and composition (Haugen et al., 2022). The time resolution of the measurements from the DISCmini is 1 s.
- Aethlabs microAeth AE51, which is a real-time BC monitor in the range between 0 – 1 mg BC/m^3 , with a measurement precision of $\pm 0.1 \mu\text{g BC/m}^3$. This is done by measuring the rate of change in absorption of transmitted light (wavelength at 880 nm) due to continuous collection of aerosol deposit on the filter within the device. Measurements can be collected in different time resolutions starting from 1 s. Following the settings suggested by the manufacturer for the specific environment and conditions, a 1-minute resolution was chosen.

These sensors were fit within a backpack (total weight is less than 3 kg), and they were connected to silicone tubes (about 20 cm long) facing the right side of the backpack (figure

S1. Additionally, a Bosch BME-280 sensor was fit next to the OPC-N3 inlet for continuous monitoring of the temperature and RH, as well as a GSM module for real time monitoring and reporting of the measurements to the cloud. All measurements in the present study were averaged to a 1-minute resolution for consistency. The backpack was designed so the volunteer citizen scientists could conduct their day as normal with plenty of space left for the bag to be used to carry their belongings.

2.2 Calibration

All sensors were collocated with the research grade instruments at the Birmingham Air Quality Supersite (BAQS) at the University of Birmingham (Bousiotis et al., 2021) and about 1 km north of the study area. Two collocation periods, before and after the campaign, of a total of about 4 days were done, in which the inlets of the sensors were placed next to the inlets of the research grade instruments at BAQS for simultaneous measurements. For the OPC-N3, after removing the outliers, an exponential relationship was considered between the ratio of the measurements of the sensor and the research grade instrument and the relative humidity (RH) in the atmosphere. The precision of the low-cost sensors, and especially those that measure particle concentrations, is known to be greatly affected by atmospheric conditions and especially RH. As a result, an overestimation of the $PM_{2.5}$ and the PM_{10} concentrations from the sensor is observed with higher RH due to PM hygroscopicity effects (Crilley et al., 2020, 2018; Khreis et al., 2022). While this is a common feature of the meteorological conditions in the United Kingdom, the RH during the campaign was rather low reducing the discrepancy found between the measurements of the sensors and the actual atmospheric conditions. Nevertheless, the calibration greatly improved the precision of the measurements especially for the larger $PM_{2.5}$ and PM_{10} (Pearson correlation $r_{PM_{10}} = 0.81$ to 0.84 , $r_{PM_{2.5}} = 0.63$ to 0.75 , $r_{PM_{10}} = 0.32$ to 0.57).

The measurements of the microAeth AE51 were calibrated against those from the MAGEE Scientific aethalometer AE33 located at the BAQS. As the BC sensor was not significantly affected by the meteorological conditions during the campaign, a linear relationship was found between the measurements of the sensor and the scientific instrument ($r = 0.65$). The low-cost sensor on average overestimated the BC concentrations by a factor of 1.75. This

discrepancy was corrected after the calibration also leading to a slight improvement of the correlation between the two datasets ($r = 0.66$).

The DISCmini was calibrated against the TSi CPC 3775 located at the BAQS. The CPC 3775 is a research grade instrument which measures particles in the size range 4 nm up to 3 μm . As the DISCmini measures the total particle number in a fraction of this size range, its collocation measurements were calibrated against the adjusted total particle number from the CPC 3775, considering only the size range that is common between the two instruments.

Finally, the measurements of the meteorological sensor were also calibrated against those from the Elms Road meteorological station at the University of Birmingham. As the sensor is located inside the container of the OPC, its values are different from the atmospheric ones, with the RH being underestimated and the temperature overestimated. Regardless, the correlation between the sensor's and atmospheric values was very high ($r > 0.95$), thus a simple linear regression was sufficient for the calibration of the measurements. Finally, the traffic data for Bristol Road were provided by the Birmingham City Council.

2.3 Positive Matrix Factorisation and estimated PM contribution calculation

The Positive Matrix Factorisation is a multivariate data analysis method developed by (Paatero and Tapper, 1994, 1993), which has been successfully applied numerous times for receptor modelling studies for source apportionment with atmospheric data (Beddows et al., 2015; Cesari et al., 2016; Rivas et al., 2020). It considers the measured data of different variables for each timestep and their experimental uncertainties as an input. The uncertainties for the equipment used in the present study range between 15-25% according to manufacturers' specifications and previous studies (Alas et al., 2020; Alphasense, 2019b; Bau et al., 2015). These were used in the present study ensuring that the Q to $Q_{\text{theoretical}}$ ratio is as close to 1 as possible. The outputs are a matrix of factors (F), which represent the average values associated with the different factors, a matrix of their contributions (G) for each timestep of the dataset provided, and a matrix of residuals (E) (the non-explained by the method part of the variation of the variables) using a least-squares technique (Reff et al., 2007). The matrices F and G are determined so that the Euclidean norm of the matrix of residuals divided by the experimental uncertainties is minimised. The PMF is a descriptive

model, thus has no objective criterion for the optimal number of factors (Paatero et al., 2002).

Thus, the optimal solution is chosen by the user depending on:

- The ability to understand what each factor represents
- The uniqueness of the factors generated (having low correlations between their variation)
- The significance of the factors (factors with near zero contribution to all the atmospheric variables were not considered)
- The reduction (as much as possible) of the unexplained variance.

The estimated PM concentrations reported are calculated using the F and G values provided by the model. As $F_{(i)}$ represents the average contribution of each variable for each factor and $G_{(i)}$ represents the contribution of each factor at a given timestep (normalised to one), the estimated PM concentrations are calculated as:

$$PM_{est(i)} = F_{PM(i)} \times G_{(i)}$$

This calculation also considers the non-explained variance from the factors in the analysis, as this is also included in the outputs of the model. While this method does not provide an accurate value for each variable at each timestep, as it considers the average contribution of all variables in a factor to vary as one (according to the single G contribution for each factor), it has been proven successful in providing a sensible portrayal of the effect of the different factors on the air quality conditions and provide a reliable estimation for the PM concentrations of the different factors (Bousiotis et al., 2023a).

For the PMF analysis, the second iteration of PMF software was used, developed by (Paatero, 2004). Further analysis of the results was done using the Openair package for R developed by (Carslaw and Ropkins, 2012).

3. RESULTS

3.1 General conditions

The campaign took place during the period between the 15/6/2023 to 26/6/2023 within the Selly Oak area in the city of Birmingham, UK. Selly Oak is predominantly populated by students within higher education and is located directly south of the University of Birmingham. This campaign coincided with the end of the term at the University of Birmingham, and while many

students still live in the area, the landlords take advantage of the relatively quiet period to conduct construction and renovation works upon the houses for the next academic year. Locations of construction work were pinpointed during the walks and are highlighted within Figure 1. During the measurement campaign period relatively high temperatures for the location and season occurred ($18.9\pm 3.7^\circ\text{C}$), the average relative humidity was $66.9\pm 29.9\%$ and there were no rainy days. Moderate winds ($2.2\pm 1.9\text{ m s}^{-1}$) were experienced during the campaign period, with wind direction predominantly from the ENE and SW directions.

The average pollutant concentrations of PM_{10} , $\text{PM}_{2.5}$, PM_{10} and black carbon (BC), and their relationship with wind direction and time of the day, measured at the nearby Birmingham Air Quality Supersite (BAQS), are shown in Figure 2. The wind conditions clearly affect the pollutant concentrations, as more polluted conditions occur from the NE which corresponds to air from the direction of the city centre. The time of the day also affects pollutant concentrations, with BC particularly affected by morning and evening rush hours.

The average pollutant and wind conditions for each of the citizen science walks are given in Table 1. Walks during the days with easterly winds have the highest PM concentrations. Furthermore, morning walks presented the higher average concentrations of the pollutants compared to other time periods.

3.2 Source apportionment

Source apportionment using the PMF algorithm was performed on the collected air pollution dataset. Particle counts per size bin and the PM mass concentrations were obtained from OPC-N3 optical particle counters, the eBC data from microaethalometers and the PN and LDSA from the DISCmini devices. Solutions with different numbers of factors were attempted and a 5-factor solution was considered optimal to describe the different sources of air pollution in the area, ensuring the unique nature of the factors formed (Figure S2). The particle number size distribution (PNSD) profiles for the different factors are found in Figure S3. The average contribution of each factor on the PM, BC, PN and LDSA is presented in the Table 2 and the contribution of each factor for different wind conditions is shown in Figure 3. Furthermore, Figure 4 shows the average contribution of each factor for each block in a 12x12

grid (representing 0.001'x0.001' longitude x latitude). In this case, the grid presentation was chosen as these are not measured values but the output of the model, representing the average conditions in each block.

The first factor presents a strong contribution to the PM_{10} , $PM_{2.5}$ and BC concentrations, while a less significant association with the LDSA was also observed. The lower PM_{10} concentration found for this factor indicates the lack of coarse particles associated with the source. This factor is largely invariant for most wind directions and speeds, however, a clear peak is observed with winds from the NE. Looking at the temporal variation of this factor (Table S1), higher contributions of this factor were observed during the morning walks, especially on the days with easterly winds, regardless of the weekday. This factor is assigned as an urban background factor, which includes the homogenized effect of the urban sources outside the study area, mainly from the direction of the city centre of Birmingham located about 3 km to the east of the study area, as well as from other urban areas surrounding the study site.

The second and fourth factors have similar characteristics, presenting a contribution from larger sized PM, especially in the PM_{10} fraction, while their association and effect on the BC and PM_{10} is negligible. The almost exclusive effect of these factors on the larger PM sizes explains the minimal effect these factors had on the total PN. Both factors present higher contributions from the highly residential parts of the study area, see Figure 4, and lower contributions on the perimeter of the Selly Oak area (Table S2), with few exceptions. These are mostly associated with possible emissions from the train station at the western side of the block as well as the grill restaurants located at the Raddlebarn Road on the southern side, which appear to affect both factors. Cooking emissions may also be included in this factor, especially close to restaurants. Though several solutions were tested, none of them introduced a clear cooking factor in the area. Increased contributions to the factors are observed at several specific points within the study area. Specifically, for the second factor, these often coincide with locations where construction activities were being undertaken. It is interesting to note, that while the correlation between Factor 2 and Factor 4 is relatively high ($r = 0.66$), they present different spatial hot-spots and behaviours. Factor 2, which is a more PM_{10} focused factor ($PM_{2.5}/PM_{10} = 0.06$ and 0.19 for F2 and F4 respectively), has sharper peaks and faster decay times compared to the Factor 4, as well as time periods and areas with

no presence at all. Factor 4 has a more constant presence with less intense peaks. This probably explains the greater and more focused peaks found on the map for Factor 2 and indicate its more hyperlocal nature compared to the Factor 4. This is consistent with (Frederickson et al., 2022) who discussed the correlation between the fluctuation of the presence and effect of a source and its regionality.

The third factor provides a contribution to all the PM sizes. Its effect seems to be more significant for PM_{2.5}, for which it is the greatest contributor in the study area. Its variation with the wind is minimal, with the sole exception for SW winds for which its contribution is almost doubled. Looking at the PNSD profile for this factor, two peaks appear in the sizes around 750 nm and 2 µm. This particle profile is similar to the ones consistently found in previous source apportionment studies in the UK, presented similar characteristics and was associated with the dominant effect of marine sources, due to the ocean surrounding the British islands (Bousiotis et al., 2023b, 2022). As expected, this factor had higher average contribution for the days with strong SW winds, while smaller variations were found between day of the week or hour of the day. This factor is assigned as the marine factor.

The fifth factor is of great interest, as for the first time to the authors' knowledge, a source apportionment study using LCS clearly identifies the effect of traffic. While the variation of the contribution of this factor with the wind seems to be minimal, a small increase is observed with northerly winds, emphasised by the great difference in its contribution between days with NE winds against those with SW (Table S1). This is expected, as the traffic flux is much greater for the two main roads (Bristol and Raddlebarn roads) and especially the Bristol Road located at the northern end of the study area (about 800 vehicles/hour during the measuring campaign hours). This factor has a rather small effect on all the PM size ranges, but a strong association was found with the BC concentrations, the PN and the LDSA. The combination of the strong effect on the PN but limited on the PM₁ further establishes its traffic nature, as the vehicle emissions from the tailpipe are mostly below the measuring capabilities of the OPC (Beddows et al., 2023; Kittelson et al., 2003). It is also notable that the association of this factor with the LDSA and the PN is better established compared to that with the BC. This is in agreement with the findings of Chang et al., (2022), who reported that the relationship of these two variables with the traffic flux is greater than that of the BC. In our study, BC was

almost equally attributed to the urban background and the traffic factors, while only a small portion was associated with other sources. The relationship of this factor with traffic is also visible in figure 4, in which we can see the high contributions at the Bristol Road (a very busy road on the northern part of the study area) as well as to a lesser extent at the Raddlebarn Road (the horizontal road on the southern end of the study area). This factor is assigned as the local traffic factor.

3.3 Spatial source separation

The separation of the sources that contribute to local air quality can provide focus to the actions required to control them. In the previous section, five distinct sources of pollution have been identified. Factors 1 and 3 represent regional sources that are clearly associated with specific wind directions and are less affected by diurnal variations. Factors 2, 4 and 5 were found to have more local characteristics. Factor 5 is easily assigned as a local traffic source. Factors 2 and 4 appear to be associated with sources specifically within the study area. Assigning the factors identified to the local (F2, F4 and F5) and regional sources (F1 and F3) allows for the assessment of air quality actions required (Table 3). Starting with PM_{10} , only a small fraction of the total concentrations is associated with local sources (6.6%), showing their largely regional character. However, PM_{10} is very different to the total PN, as they were mostly assigned to the traffic factor (F5 = 82%). This is in agreement with Rivas et al., (2020)68 who found similar traffic contributions to the ultrafine particles in London's urban environment. Similar are the results for the association of the sources with the LDSA, with the local sources having the greatest contribution, largely due to traffic factor (F5), which according to our analysis was responsible for about 67% of the total LDSA contributions.

It is highlighted, this study has insufficient data to provide an assessment of the air quality within the study area either at the annual or daily timescales. The walk data are not continuous and hence cannot be used for daily averages and miss the night-time completely. The total campaign was significantly less than a year and hence cannot be used for annual averages. Thus, the comparisons presented hereafter are not to be used for general air quality assessment, but rather to provide a scale to understand the effect of different factors.

With respect to $PM_{2.5}$, the regional sources of $PM_{2.5}$ alone are greater than the annual WHO recommendations⁵ during the measurement hours, though significantly lower than the daily limits (the annual and daily $PM_{2.5}$ recommendation by WHO are 5 and 15 $\mu\text{g m}^{-3}$ respectively). The contribution of the regional sources was more than 80% of the total $PM_{2.5}$ concentrations explained by the model, making them the most important contributor for the $PM_{2.5}$ pollution. The results are different for the PM_{10} though. While the average PM_{10} concentrations are greater than the annual WHO guideline as well, these values are largely driven by the local sources of particles rather than the regional, with a contribution of more than 60%. Finally, BC is associated with both the urban background and traffic results with an almost equal contribution of local and regional sources to the total BC concentrations.

It is noted that about 20% of the PM_{10} concentrations and 30% of the BC concentrations were not explained by the model. This means that these percentages of the PM_{10} and BC were not assigned to any of the factors and thus their sources cannot be pinpointed. This along with the very low contribution of the Urban Background (F1) on the coarse particle ($PM_{2.5-10}$) concentrations may be the reason of the regional (as well as that of the F1) PM_{10} contribution erroneously appearing lower than that of the $PM_{2.5}$ on the present analysis. Solutions with a greater number of factors were attempted but did not improve the performance of the model for these two variables. As the PMF does not comprehend the inherent relations between the variables inputted, such discrepancies may occur. Furthermore, the possibility that the high uncertainties due to the nature of the low-cost sensors may also be responsible for these discrepancies cannot be ruled out. These points should be considered for future studies.

Looking at the effect of the regional factors compared to the local ones, we see the effect of the urban background to be greater in the perimeter of the Selly Oak residential area (Table S2). Almost all roads in the perimeter present average contributions of the first factor that are greater than 1, which means that the effect of that factor is greater than average for these roads. On average, the effect of the urban background is about 20% greater at the perimeter of the block compared to the inner parts of the block. This is probably the result of the lower density urban landscape surrounding the Selly Oak residential area, compared to the densely built space within it, which may reduce the relative effect of the more regional sources. The only exception to this is the Raddlebarn Road for which, while the effect is greater than most

of the inner roads, is smaller than the average. A possible explanation for this is the Selly Park, located south of that road, which may have a reducing effect of the incoming urban background emissions due to the presence of trees. In contrast, the local factors present greater contributions within the block compared to the perimeter. By averaging the contribution of the factors per grid point included on each road in the study area, we were able to compare the effect of the local sources between them. The more PM_{10} -focused F2 and F4 were found to be about 12-14% greater on the roads within the block compared to those at the perimeter. Finally, the effect of the traffic factor is about 60% greater for the perimeter of the block compared to the inner part (Table S2). As explained earlier, while the inner roads have some traffic activity, this is a lot less than that of the outer roads and especially Bristol Road, which presents the greatest contribution for this factor. Additionally, looking at the standard deviation of the different factors among the roads, we can see that the variation is a lot greater for the local factors compared to the regional ones. This is an expected result as the variability of the regional sources is a lot lower and its effect is expected to be more balanced throughout the block due to their nature.

3.4 Mapping an area

Mobile campaigns can be very useful for air quality studies as they provide data at a hyperlocal resolution. We now show that source apportionment methodologies can be used to generate hyperlocal source apportionment. Maps of the average concentrations for the different spots within the study area during our campaign are found in Figure 5.

From Figure 5, great variability in the different pollutants can be observed. For the regulatory important $PM_{2.5}$ and PM_{10} , higher mass concentrations are found mostly within the Selly Oak block. According to the analysis presented in the previous section, the sources associated with such emissions have a more local character and appear to have a greater effect especially on the PM_{10} within the block compared to the perimeter areas. This though provides only a limited image of the health risk that exists for the different areas of the block. The LDSA, a metric that provides valuable information for health effect studies but is not regulated, shows the greater risk found on the perimeter of the block and mainly the northern side where the Bristol Road is, as well as on the busy junctions at the NW and SE of the study area. As

highlighted earlier in the source apportionment analysis, the emissions in that road are mainly of traffic nature which, due to their size and chemical composition, may be associated with the most adverse health effects.

Furthermore, the combination of the mobile measurements and the source apportionment analysis can provide information about the evolution of the different sources, and the range of their effect. An example of such an analysis is found in Figure 6, in which the 10 points traversing Dawlish Road, the North - South of the block, can be assessed both for the average concentrations of the $PM_{2.5}$, PM_{10} and LDSA, as well as the partial effect of each factor on them. For the $PM_{2.5}$ we can see that the most important sources are the regional ones, with an (as expected) almost equal effect across the whole road. This changes for the PM_{10} , for which local sources appear to be more influential in its variation, with the highest contribution being that of F4. It is notable that two of the peaks of the contribution of F4 on that road appear close to the points where construction work is undertaken and the PM_{10} concentrations are expected to be increased (Hong et al., 2020; Sekhavati and Yengejeh, 2023). Finally, for the LDSA, the profile is completely different. While there is almost a consistent value within the block, we can see an increase on the edges, where the road meets the two main traffic roads in the block. For this edge effect, it is the variation of the traffic factor (F5) that contributes the most significantly.

A similar analysis was done for the Bristol Road, which is the main traffic road within the study area. The profile of the $PM_{2.5}$, PM_{10} and LDSA are found in Figure 7. The most interesting variation for this road is within the LDSA, which is directly associated to traffic emissions. The LDSA average values are almost double to those observed at Dawlish Road (Figure 6). The peaks found coincide either with the traffic lights in the area, or near the junction at the western end of the road which has no traffic light there. For these specific points, the LDSA values associated with the traffic factor are almost 150% greater than those for the whole Bristol Road and more than 200% greater than the peak points found in Dawlish Road.

The same analysis was done for the rest of the roads as well, mapping the different sources and their effect within the study area. The results of this analysis are presented in the SI figures S4a, b. Looking at the detailed analysis of each one of the roads, the effect of several point or area sources, such as the train station at Heeley Road (H3 to H6), the restaurants at

Raddlebarn Road (R3), the junctions at both ends of Bournbrook Road (O1 and O10), or the local PM_{10} hotspots, mainly attributed to variations of F2 and F4 and once again coinciding in some cases at points where construction activities were undertaken (e.g. around T8 in Tiverton Road or S4 and S6 in Harrow Road).

The results from the source apportionment analysis of mobile monitoring data show the great potential of the methodology in providing not only a detailed map of pollution hotspots, but also the attribution of different sources to the hot spots.

4. DISCUSSION

In this paper, we show that LCS mobile monitoring and source apportionment can be used to generate a wealth of air quality data that can pinpoint air pollution sources without the need of extensive or expensive campaigns. This level of detail is not possible with static networks. Hence, mobile LCS provide the opportunity to dramatically extend the existing regulatory network due to their low cost and portability. Through a relatively small number of citizen science enabled mobile monitoring walks we have been able to map and highlight air pollution hotspots and sources relevant to thousands of people living within a highly urbanized area.

Previous studies using static monitoring locations have successfully identified the importance of regional sources of PM pollution. This study highlights that mobile measurements can identify hyperlocal pollution hot spots in addition to regional sources with a significantly reduced cost. Hyperlocal sources such as construction sites or road junctions typically only influence local air quality over a short range, but their impact can be significant since the study area is densely populated.

The mobile source apportionment approach allows for the relative importance of the different sources on the local environment to be assessed. Through this information, better urban planning and governance is possible, as the method provides the information needed to assess the relative importance of different sources. It is noted that some sources identified are not important from a regulatory PM perspective which currently only considers $PM_{2.5}$ and

PM₁₀ mass concentrations. However, PM₁, PN and LDSA have consistently been shown to be important for public health. For example, the traffic factor (Factor 5) from our analysis is not “visible” if one just looks at PM_{2.5} and PM₁₀ mass concentrations, but it is significant from a PN and LDSA perspective which are indicative of smaller particles that contribute little to PM_{2.5} and PM₁₀ mass concentrations. The traffic factor which appears to have hot spots within the study area, even though it is present almost throughout the study area, plays a decisive role on the variation of the pollutants associated with smaller particles. The negative effect of smaller particles upon public health are well documented (Chang et al., 2022; Schmid and Stoeger, 2016). Several studies have suggested that in many cases the mass concentration of particles can be of lesser importance in comparison to the number of particles or their surface area (Schmid and Stoeger, 2016).

Our study shows that mobile LCS monitoring with citizen scientists provides an affordable and versatile approach to providing air pollution information services. Going forward, the mobile monitoring can be combined with readily available public information on socio-economic data (population density, traffic flow, etc.) and meteorological variables to generate a digital twin of the causes and effects of local air pollution. This will provide information at a local scale that can influence both governance and public understanding of air pollution and provide information on how to reduce and avoid air pollution exposure.

The method presented comes with certain limitations. The citizen science walks provide only a snapshot of the pollution profile at the given times and locations of each walk. In many cases, significant sources of pollution were not identified in walks made at different times of the day. For example, the effect of construction works is greatly reduced when presenting the average of all the walks, as construction typically only occurs during the working day. A solution to this would be to engage more citizen scientists to take more walks at different times of the day, but this would have implications upon OpEx costs.

In our study, we achieved the mapping of sources and their relative importance with only 10 citizen science walks. The approach can be translated and expanded to other locations. Future studies should be tailored according to the specific needs in each case. For example, our analysis does not cover possible sources during night hours since no walks were taken during

this period. The approach could be used to provide additional information to regulatory networks. Crowd collected measurements reduce OpEx costs, and LCS reduce CapEx costs. The Internet of Things (IoT) methodologies needed for such work are already available (Kortoçi et al., 2022; Robinson et al., 2018). The outputs from fast and flexible campaigns, combined with the results from the existing network can greatly improve and extend the capabilities for pollution monitoring and control and increase our understanding of local air pollution, actively engaging the public and help in the improvement of the air quality for everyone.

5. CONCLUSIONS

In the present study, a novel methodology is presented using only a handful of mobile measurements collected by low-cost sensors, measuring PM, BC, total particle number and LDSA, to identify and quantify the effect of the sources influencing these in a residential area of Selly Oak, Birmingham, UK. The methodology successfully identified the mix of regional and local sources affecting the air quality in the area with multiple proportions depending on the area, time of the day, weekday and synoptic conditions. In most cases, the PM concentrations found were higher than the hourly averages suggested by the WHO, though significantly lower than the annual suggested averages. For these averages it should be considered that all measurements were done during daytime, which points that the daily averages are expected to be significantly lower. Five distinct sources of pollution were identified using the PMF, three of which had a more local character while the other two were associated with sources further outside from the block. Regional sources had a greater effect on the smaller PM_1 and $PM_{2.5}$ concentrations, while PM_{10} concentrations were mainly driven by local sources (more than 60%). Among the sources found the traffic factor was identified for the first time in a study using low-cost sensors. Its effect was not significant on the PM, but greatly increased the total particle number as well as the LDSA, a metric that measures the effect of small particles on the respiratory system and is barely captured by the currently regulated metrics. Due to this discrepancy, the shortcomings of using just the $PM_{2.5}$ and PM_{10} concentrations for regulatory studies especially in urban areas is illustrated. Our study showed that some parts of the study area did not have significant concentrations of the regulated PM, but were directly affected by the traffic emissions, and could falsely be considered as within safe limits. In a similar manner, our study pointed the limitations that

come with the existing measuring network to capture the significant variations of the larger particles from hyperlocal sources that extend only to a limited area. Even though the concentrations of PM_{2.5} and PM₁₀ are considered to barely vary in such small areas, our results showed that the effect of these hyperlocal sources only extend to a couple of hundred meters, still affecting the air quality for hundreds of people in such a densely populated area. While studies like this can provide crucial information in dealing with hyperlocal air quality problems, extra care should be taken on their design to provide a realistic and non-biased result. Thus, more similar studies in different scenarios should be done to improve their capabilities and extend their usage.

DATA AVAILABILITY

The datasets generated and/or analysed during the current study are available in the UBIRA repository, <https://doi.org/10.25500/edata.bham.00001029>

CODE AVAILABILITY

The data analysis in the present study was carried out using both open source and proprietary software. While the proprietary software is available from its corresponding author, the code used with the open-source software is available from D.B. (d.bousiotis@bham.ac.uk) upon reasonable request.

REFERENCES

- Alas, H.D.C., Müller, T., Weinhold, K., Pfeifer, S., Glojek, K., Gregorič, A., Močnik, G., Drinovec, L., Costabile, F., Ristorini, M., Wiedensohler, A., 2020. Performance of microaethalometers: Real-world field intercomparisons from multiple mobile measurement campaigns in different atmospheric environments. *Aerosol Air Qual Res* 20, 2640–2653. <https://doi.org/10.4209/aaqr.2020.03.0113>
- Alexeeff, S.E., Roy, A., Shan, J., Liu, X., Messier, K., Apte, J.S., Portier, C., Sidney, S., Van Den Eeden, S.K., 2018. High-resolution mapping of traffic related air pollution with Google street view cars and incidence of cardiovascular events within neighborhoods in Oakland, CA. *Environ Health* 17, 1–13. <https://doi.org/10.1186/s12940-018-0382-1>

- Alfano, B., Barretta, L., Giudice, A. Del, De Vito, S., Francia, G. Di, Esposito, E., Formisano, F., Massera, E., Miglietta, M.L., Polichetti, T., 2020. A review of low-cost particulate matter sensors from the developers' perspectives. *Sensors (Switzerland)* 20, 1–56. <https://doi.org/10.3390/s20236819>
- Alphasense, 2019a. User Manual for OPC-N3 Optical Particle Counter. Alphasense Ltd., Essex, UK.
- Alphasense, 2019b. User Manual for OPC-N3 Optical Particle Counter. Alphasense Ltd., Essex, UK.
- Anastasiou, E., Vilcassim, M.J.R., Adragna, J., Gill, E., Tovar, A., Thorpe, L.E., Gordon, T., 2022. Feasibility of low-cost particle sensor types in long-term indoor air pollution health studies after repeated calibration, 2019–2021. *Sci Rep* 12, 1–8. <https://doi.org/10.1038/s41598-022-18200-0>
- Apparicio, P., Gelb, J., Jarry, V., Mann, É.L., 2021. Cycling in one of the most polluted cities in the world : Exposure to noise and air pollution and potential adverse health impacts in Delhi. *Int J Health Geogr* 1–16. <https://doi.org/10.1186/s12942-021-00272-2>
- Austin, E., Novosselov, I., Seto, E., Yost, M.G., 2015. Laboratory evaluation of the Shinyei PPD42NS low-cost particulate matter sensor. *PLoS One* 10, 1–17. <https://doi.org/10.1371/journal.pone.0137789>
- Bau, S., Zimmermann, B., Payet, R., Witschger, O., 2015. A laboratory study of the performance of the handheld diffusion size classifier (DiSCmini) for various aerosols in the 15-400 nm range. *Environmental Sciences: Processes and Impacts* 17, 261–269. <https://doi.org/10.1039/c4em00491d>
- Beddows, D.C.S., Harrison, R.M., Gonet, T., Maher, B.A., Odling, N., 2023. Measurement of road traffic brake and tyre dust emissions using both particle composition and size distribution data. *Environmental Pollution* 331, 121830. <https://doi.org/10.1016/j.envpol.2023.121830>
- Beddows, D.C.S., Harrison, R.M., Green, D.C., Fuller, G.W., 2015. Receptor modelling of both particle composition and size distribution from a background site in London, UK. *Atmos Chem Phys* 15, 10107–10125. <https://doi.org/10.5194/acp-15-10107-2015>
- Belis, C.A., Favez, O., Mircea, M., Diapouli, E., Manousakas, M.-I., Vratolis, S., Gilardoni, S., Paglione, M., Decesari, S., Mocnik, G., Mooibroek, D., Salvador, P., Takahama, S., Vecchi, R., Paatero, P., European Commission. Joint Research Centre., n.d. European guide on air pollution source apportionment with receptor models : revised version 2019.
- Birnbaum, H.G., Carley, C.D., Desai, U., Ou, S., Zuckerman, P.R., 2020. Measuring the impact of air pollution on health care costs. *Health Aff* 39, 2113–2119. <https://doi.org/10.1377/hlthaff.2020.00081>
- Boogaard, H., Kos, G.P.A., Weijers, E.P., Janssen, N.A.H., Fischer, P.H., Zee, S.C. Van Der, Hartog, J.J. De, Hoek, G., 2011. Contrast in air pollution components between major streets and background locations : Particulate matter mass , black carbon , elemental composition , nitrogen oxide and ultra fine particle number. *Atmos Environ* 45, 650–658. <https://doi.org/10.1016/j.atmosenv.2010.10.033>
- Bousiotis, D., Alconcel, L.N.S., Beddows, D.C.S., Harrison, R.M., Pope, F.D., 2023a. Monitoring and apportioning sources of indoor air quality using low-cost particulate matter sensors. *Environ Int* 174, 107907. <https://doi.org/10.1016/j.envint.2023.107907>
- Bousiotis, D., Allison, G., Beddows, D.C.S., Harrison, R.M., Pope, F.D., 2023b. Towards comprehensive air quality management using low-cost sensors for pollution source

- apportionment. *NPJ Clim Atmos Sci* 6, 1–10. <https://doi.org/10.1038/s41612-023-00424-0>
- Bousiotis, D., Beddows, D.C.S., Singh, A., Haugen, M., Diez, S., Edwards, P.M., Boies, A., Harrison, R.M., Pope, F.D., 2022. A study on the performance of low-cost sensors for source apportionment at an urban background site. *Atmos Meas Tech* 15, 4047–4061. <https://doi.org/10.5194/amt-15-4047-2022>
- Bousiotis, D., Singh, A., Haugen, M., Beddows, D.C.S., Diez, S., Murphy, K.L., Edwards, P.M., Boies, A., Harrison, R.M., Pope, F.D., 2021. Assessing the sources of particles at an urban background site using both regulatory instruments and low-cost sensors – a comparative study. *Atmos Meas Tech* 14, 4139–4155. <https://doi.org/10.5194/amt-14-4139-2021>
- Buehler, C., Xiong, F., Levy Zamora, M., Skog, K.M., Kohrman-Glaser, J., Colton, S., McNamara, M., Ryan, K., Redlich, C., Bartos, M., Wong, B., Kerkez, B., Koehler, K., R. Gentner, D., 2021. Stationary and portable multipollutant monitors for high-spatiotemporal-resolution air quality studies including online calibration. *Atmos Meas Tech* 14, 995–1013. <https://doi.org/10.5194/amt-14-995-2021>
- Bulot, F.M.J., Russell, H.S., Rezaei, M., Johnson, M.S., Ossont, S.J.J., Morris, A.K.R., Basford, P.J., Easton, N.H.C., Foster, G.L., Loxham, M., Cox, S.J., 2020. Laboratory comparison of low-cost particulate matter sensors to measure transient events of pollution. *Sensors (Switzerland)* 20. <https://doi.org/10.3390/s20082219>
- Carslaw, D.C., Ropkins, K., 2012. openair — An R package for air quality data analysis. *Environmental Modelling & Software* 27–28, 52–61. <https://doi.org/10.1016/j.envsoft.2011.09.008>
- Cesari, D., Amato, F., Pandolfi, M., Alastuey, A., Querol, X., Contini, D., 2016. An inter-comparison of PM₁₀ source apportionment using PCA and PMF receptor models in three European sites. *Environmental Science and Pollution Research* 23, 15133–15148. <https://doi.org/10.1007/s11356-016-6599-z>
- Chang, P.K., Griffith, S.M., Chuang, H.C., Chuang, K.J., Wang, Y.H., Chang, K.E., Hsiao, T.C., 2022. Particulate matter in a motorcycle-dominated urban area: Source apportionment and cancer risk of lung deposited surface area (LDSA) concentrations. *J Hazard Mater* 427, 128188. <https://doi.org/10.1016/j.jhazmat.2021.128188>
- Chatzidiakou, L., Krause, A., Popoola, O., Di Antonio, A., Kellaway, M., Han, Y., Squires, F., Wang, T., Zhang, H., Wang, Q., Fan, Y., Chen, S., Hu, M., Quint, J., Barratt, B., Kelly, F., Zhu, T., Jones, R., 2019. Characterising low-cost sensors in highly portable platforms to quantify personal exposure in diverse environments. *Atmos Meas Tech* 12, 4643–4657. <https://doi.org/10.5194/amt-12-4643-2019>
- Coelho, S., Ferreira, J., Lopes, M., 2023. Source apportionment of air pollution in urban areas: a review of the most suitable source-oriented models. *Air Qual Atmos Health* 16, 1185–1194. <https://doi.org/10.1007/s11869-023-01334-z>
- Crilly, L.R., Shaw, M., Pound, R., Kramer, L.J., Price, R., Young, S., Lewis, A.C., Pope, F.D., 2018. Evaluation of a low-cost optical particle counter (Alphasense OPC-N2) for ambient air monitoring. *Atmos Meas Tech* 11, 709–720. <https://doi.org/10.5194/amt-11-709-2018>
- Crilly, L.R., Singh, A., Kramer, L.J., Shaw, M.D., Alam, M.S., Apte, J.S., Bloss, W.J., Hildebrandt Ruiz, L., Fu, P., Fu, W., Gani, S., Gatari, M., Ilyinskaya, E., Lewis, A.C., Ng'ang'a, D., Sun, Y., Whitty, R.C.W., Yue, S., Young, S., Pope, F.D., 2020. Effect of

aerosol composition on the performance of low-cost optical particle counter correction factors. *Atmos Meas Tech* 13, 1181–1193. <https://doi.org/10.5194/amt-13-1181-2020>
 deSouza, P., Anjomshoa, A., Duarte, F., Kahn, R., Kumar, P., Ratti, C., 2020. Air quality monitoring using mobile low-cost sensors mounted on trash-trucks: Methods development and lessons learned. *Sustain Cities Soc* 60.

<https://doi.org/10.1016/j.scs.2020.102239>

Forouzanfar, M.H., Alexander, L., Bachman, V.F., Biryukov, S., Brauer, M., Casey, D., Coates, M.M., Delwiche, K., Estep, K., Frostad, J.J., Astha, K.C., Kyu, H.H., Moradi-Lakeh, M., Ng, M., Slepak, E., Thomas, B.A., Wagner, J., Achoki, T., Atkinson, C., Barber, R.M., Cooperrider, K., Dandona, L., Dicker, D., Flaxman, A.D., Fleming, T.D., Foreman, K.J., Gakidou, E., Hay, S.I., Heuton, K.R., Iannarone, M.L., Ku, T., Larson, H.J., Lim, S.S., Lopez, A.D., Lozano, R., MacIntyre, M.F., Margono, C., McLain, A., Mokdad, A.H., Mullany, E.C., Murray, C.J.L., Naghavi, M., Nguyen, G., Pain, A.W., Richardson, L., Robinson, M., Sandar, L., Stephens, N., Temesgen, A.M., Thomson, B., Vos, T., Wan, X., Wang, H., Wurtz, B., Ebel, B.E., Ellenbogen, R.G., Wright, J.L., Alfonso-Cristancho, R., Anderson, B.O., Jensen, P.N., Quistberg, D.A., Riederer, A., Vavilala, M.S., Zunt, J.R., Anderson, H.R., Pourmalek, F., Gotay, C.C., Burnett, R., Shin, H.H., Weichenthal, S., Cohen, A., Knudsen, A., Aasvang, G., Kinge, J.M., Skirbekk, V., Vollset, S., Abbafati, C., Abbasoglu Ozgoren, A., Çavlin, A., Kucuk Bicer, B., Abd-Allah, F., Abera, S.F., Melaku, Y.A., Aboyans, V., Abraham, B., Puthenpurakal Abraham, J., Abraham, J.P., Thorne-Lyman, A.L., Ding, E.L., Fahimi, S., Khatibzadeh, S., Wagner, G.R., Bukhman, G., Campos-Nonato, I.R., Feigl, A.B., Salomon, J.A., Benzian, H., Abubakar, I., Abu-Rmeileh, N.M.E., Aburto, T.C., Avila, M.A., Barquera, S., Barrientos-Gutierrez, T., Campuzano, J.C., Cantoral, A.J., Contreras, A.G., Cuevas-Nasu, L., De, V., García-Guerra, F.A., Gomez Dantes, H., Gonzalez de Cosio, T., González-Castell, D., Heredia-Pi, I.B., Hernandez, L., Jauregui, A., Medina, C., Mejia-Rodriguez, F., Montañez Hernandez, J.C., Pedraza, L.S., Pedroza, A., Quezada, A.D., Salvo, D., Sanchez, L.M., Sánchez-Pimienta, T.G., Servan-Mori, E.E., Shamah Levy, T., Téllez Rojo, M.M., Villalpando, S., Adelekan, A., Adofo, K., Adou, A.K., Adsuar, J.C., Fra Paleo, U., Afshin, A., Micha, R., Mozaffarian, D., Shahrzad, S., Shangquan, S., Singh, G.M., Agardh, E.E., Al Khabouri, M.J., Al Lami, F.H., Alam, S., Naheed, A., Alasfoor, D., Albittar, M.I., Alegretti, M.A., Cavalleri, F., Aleman, A. V., Colistro, V., Alemu, Z.A., Alhabib, S., Chen, Z., Gething, P., Ali, R., Bennett, D.A., Briggs, A.D.M., Rahimi, K., Scarborough, P., Simard, E.P., Ali, M.K., Argeseanu Cunningham, S., Liu, Y., Narayan, K.M.V., Omer, S.B., Alla, F., Guillemin, F., Allebeck, P., Roy, N., Kivipelto, M., Weiderpass, E., Fereshtehnejad, S., Havmoeller, R., Sindi, S., Allen, P.J., Alsharif, U., Endres, M., Nolte, S., Papachristou, C., Alvarez, E., Alvis-Guzman, N., Paternina Caicedo, A.J., Amankwaa, A.A., Amare, A.T., Hoek, H.W., Gansevoort, R.T., Yenesew, M., Ameh, E.A., Ameli, O., Amini, H., Tanner, M., Ammar, W., Harb, H.L., Antonio, C.A.T., Faraon, E.A., Panelo, C.A., Anwari, P., Arnlöv, J., Larsson, A., Arsic Arsenijevic, V.S., Artaman, A., Asghar, R.J., Assadi, R., Atkins, L.S., Awuah, B., Laryea, D.O., Badawi, A., Bahit, M.C., Bakfalouni, T., Balakrishnan, K., Balalla, S., Feigin, V.L., Te Ao, B.J., Balu, R., Dandona, R., Goenka, S., Kumar, G., Murthy, K.S., Reddy, K., Banerjee, A., Barker-Collo, S.L., del Pozo-Cruz, B., Barregard, L., Barrero, L.H., Basto-Abreu, A.C., Batis Ruvalcaba, C., de Castro, E.F., Lopez, N., Texcalac, J.L., Basu, A., Gaffikin, L., Basu, S., Basulaiman, M.O., Memish, Z.A., Beardsley, J., Bedi, N., Bekele, T., Bell, M.L., Huang, J.J., Benjet, C., Borges, G., Gutiérrez, R.A., Orozco, R., Trasande, L., Hagan, H., Bernabé, E., Wolfe, C.D.A., Beyene, T.J., Bhala, N., Derrett, S., Bhalla, A., Jha, V., Bhutta, Z.A.,

Nisar, M.I., Bikbov, B., Bin Abdulhak, A.A., Vijayakumar, L., Chiang, P.P., Blore, J.D., Brooks, P.M., Lakshmana Balaji, A., Colquhoun, S.M., Weintraub, R.G., Blyth, F.M., Meretoja, A., Bohensky, M.A., Bora Basara, B., Yentür, G.K., Kose, M.R., Pekerici, A., Uzun, S.B., Bornstein, N.M., Bose, D., Boufous, S., Degenhardt, L., Bourne, R.R., Brainin, M., Brazinova, A., Majdan, M., Breitborde, N.J., Schöttker, B., Brenner, H., Broday, D.M., Lunevicius, R., Bruce, N.G., Dherani, M.K., Pope, D., Brugha, T.S., Brunekreef, B., Kromhout, H., Buchbinder, R., Gabbe, B., Gibney, K.B., Thrift, A.G., Bui, L.N., Nguyen, N.T., Bulloch, A.G., Patten, S.B., Tonelli, M., Wang, J., Burch, M., Burney, P.G.J., Jarvis, D.L., Rodriguez, A., Rushton, L., Soljak, M., Williams, T.N., Caravanos, J., Nash, D., Cárdenas, R., Cardis, E., Nieuwenhuijsen, M.J., Rojas-Rueda, D., Carpenter, D.O., Leung, R., Caso, V., Castañeda-Orjuela, C.A., Castro, R.E., Catalá-López, F., Chadha, V.K., Chang, J., Scott, J.G., Hoy, D.G., Knibbs, L.D., Charlson, F.J., Erskine, H.E., Ferrari, A.J., Gouda, H.N., Veerman, L.J., Whiteford, H.A., Chen, W., Zou, X., Chen, H., London, S.J., Jiang, Y., Takahashi, K., Chimed-Ochir, O., Chowdhury, R., Powles, J., Christophi, C.A., Chuang, T., Chugh, S.S., Cirillo, M., Claßen, T.K.D., Kraemer, A., Tobollik, M., Colomar, M., Cooper, C., Cooper, L.T., Coresh, J., Matsushita, K., Tran, B.X., Courville, K.J., Criqui, M.H., Stein, M.B., Damsere-Derry, J., Danawi, H., Refaat, A.H., Dargan, P.I., Davis, A., Fay, D.F.J., Schmidt, J.C., Davitoliu, D. V., Dayama, A., DeLeo, D., de Lima, G., Machado, V.M.P., Nogueira, J.R., Teixeira, C.M., Dellavalle, R.P., Deribe, K., Mekonnen, W., Des Jarlais, D.C., Dessalegn, M., deVeber, G.A., Lindsay, M.P., Hu, H., Devries, K.M., McKee, M., Pearce, N., Stöckl, H., Tillmann, T., Watts, C.H., Dharmaratne, S.D., Dokova, K., Dorsey, E.R., Driscoll, T.R., Marks, G.B., Leigh, J., Duan, L., Li, Y., Liu, S., Ma, J., Wang, L., Ye, P., Zhou, M., Liang, X., Durrani, A.M., Elshrek, Y.M., Ermakov, S.P., Soshnikov, S., Eshrati, B., Farzadfar, F., Esteghamati, A., Hafezi-Nejad, N., Sheikhabaehi, S., Sepanlou, S.G., Heydarpour, P., Sahraian, M., Rahimi-Movaghar, V., Ferri, C.P., Foigt, N., Franklin, R.C., Gamkrelidze, A., Khonelidze, I., Sturua, L., Gankpé, F.G., Gasana, E., Sabin, N., Geleijnse, J.M., Gessner, B.D., Gillum, R.F., Ginawi, I.A.M., Giroud, M., Giussani, G., Goginashvili, K., Gona, P., Goto, A., Guerrant, R.L., Terkawi, A.S., Gugnani, H.C., Gunnell, D., Gupta, R., Hagstromer, M., Halasa, Y.A., Idrisov, B.T., Hamadeh, R.R., Hammami, M., Hankey, G.J., Hao, Y., Zheng, Y., Haregu, T., van de Vijver, S., Haro, J., Hedayati, M.T., Hijar, M., Hoffman, H.J., Mensah, G.A., Sampson, U.K., Hornberger, J.C., Hosgood, H., Hsairi, M., Hu, G., Huang, C., Hubbell, B.J., Huiart, L., Racapé, L., Hussein, A., Iburg, K.M., Ikeda, N., Innos, K., Inoue, M., Kawakami, N., Shibuya, K., Islami, F., Ismayilova, S., Jacobsen, K.H., Jansen, H.A., Jassal, S.K., Jayaraman, S., Jeemon, P., Prabhakaran, D., Jiang, F., Jiang, G., Phillips, M.R., Jonas, J.B., Juel, K., She, J., Kan, H., Kany Roseline, S.S., Karam, N.E., Karch, A., Karema, C.K., Karthikeyan, G., Paul, V.K., Satpathy, M., Tandon, N., Kaul, A., Kazi, D.S., Kemp, A.H., Lotufo, P.A., Polanczyk, G. V., Santos, I.S., Kengne, A.P., Matzopoulos, R., Parry, C.D., Sliwa, K., Mayosi, B.M., Stein, D.J., Keren, A., Khader, Y.S., Ali Hassan Khalifa, S.E., Khan, E.A., Khang, Y., Kieling, C., Kim, D., Kim, S., Kim, Y., Kimokoti, R.W., Kinfa, Y., Kissela, B.M., Kokubo, Y., Kosen, S., Warouw, T.S., Kravchenko, M., Varakin, Y.Y., Krishnaswami, S., Kuate Defo, B., Kuipers, E.J., Polinder, S., Kulkarni, C., Kulkarni, V.S., Kwan, G.F., Lai, T., Lalloo, R., Lallukka, T., Shiri, R., Lam, H., Lan, Q., Lansingh, V.C., Lavados, P.M., Lawrynowicz, A.E., Leasher, J.L., Lee, J., Yoon, S., Levi, M., Liang, J., Wang, Y., Zhu, J., Lipshultz, S.E., Lloyd, B.K., Room, R., Logroscino, G., Lortet-Tieulent, J., Ma, S., Phua, H.P., Magis-Rodriguez, C., Mahdi, A.A., Malekzadeh, R., Mangalam, S., Mapoma, C.C., Masiye, F., Marape, M., Marcenes, W., Meaney, P.A., Margolis, D.J., Silberberg, D.H., Martin, R. V., Marzan, M.B., Mashal, M.T., Mason-Jones,

- A.J., Mazorodze, T.T., McKay, A.C., Mehndiratta, M., Meltzer, M., Mendoza, W., Apolinary Mhimbira, F., Miller, T.R., Mills, E.J., Mishra, S., Mohamed Ibrahim, N., Mohammad, K.A., Mola, G.L., Monasta, L., Montico, M., Ronfani, L., Moore, A.R., Morawska, L., Norman, R.E., Mori, R., Tsilimbaris, M., Moschandreas, J., Moturi, W.N., Werdecker, A., Mueller, U.O., Westerman, R., Mukaigawara, M., Nahas, Z., Naidoo, K.S., Naldi, L., Nand, D., Nangia, V., Neal, B., Nejjari, C., Neupane, S.P., Newton, C.R., Ngalesoni, F.N., Ngirabega, J.D., Nolla, J.M., Vollset, S.E., Norheim, O.F., Norrving, B., Nyakarahuka, L., Oh, I., Ohkubo, T., Olusanya, B.O., Opio, J.N., Pagcatipunan, R.S., Pandian, J.D., Park, E., Seedat, S., Pavlin, B.I., Pejin Stokic, L., Pereira, D.M., Perez-Padilla, R., Perez-Ruiz, F., Perico, N., Remuzzi, G., Trillini, M., Perry, S.A.L., Pervaiz, A., Pesudovs, K., Peterson, C.B., Petzold, M., Plass, D., Poenaru, D., Pond, C.D., Pope, C., Popova, S., Rehm, J., Prasad, N.M., Qato, D.M., Rafay, A., Rana, S.M., Ur Rahman, S., Raju, M., Rakovac, I., Rao, M., Razavi, H., Ribeiro, A.L., Velasquez-Melendez, G., Riccio, P.M., Sposato, L.A., Roca, A., Romieu, I., Straif, K., Ruhago, G.M., Sunguya, B.F., Sacco, R.L., Saha, S., Sahathevan, R., Sanabria, J.R., Sanchez-Riera, L., Sapkota, A., Saunders, J.E., Soneji, S., Sawhney, M., Saylan, M.I., Schneider, I.J.C., Schwebel, D.C., Singh, J.A., Serdar, B., Shaddick, G., Shinohara, Y., Shishani, K., Shiue, I., Sigfusdottir, I.D., Singh, A., Søreide, K., Sreeramareddy, C.T., Stapelberg, N.J.C., Stathopoulou, V., Steckling, N., Stroumpoulis, K., Swaminathan, S., Swaroop, M., Yano, Y., Sykes, B.L., Tabb, K.M., Talongwa, R.T., Tanne, D., Tavakkoli, M., Thackway, S. V., Thurston, G.D., Topouzis, F., Towbin, J.A., Toyoshima, H., Traebert, J., Trujillo, U., Tsala Dimbuene, Z., Tuzcu, E., Uchendu, U.S., Ukwaja, K.N., Van Dingenen, R., van Gool, C.H., van Os, J., Vasankari, T.J., Vasconcelos, A.N., Violante, F.S., Victorovich Vlassov, V., Waller, S.G., Wallin, M.T., Wang, W., Wessells, K., Wilkinson, J.D., Williams, H.C., Woldeyohannes, S.M., Wong, J.Q., Woolf, A.D., Xu, G., Yan, L.L., Yang, G., Yip, P., Yonemoto, N., Younis, M.Z., Younoussi, Z., Yu, C., Zaki, M.E., Zhao, Y., Zhu, S., 2015. Global, regional, and national comparative risk assessment of 79 behavioural, environmental and occupational, and metabolic risks or clusters of risks in 188 countries, 1990-2013: A systematic analysis for the Global Burden of Disease Study 2013. *The Lancet* 386, 2287–2323. [https://doi.org/10.1016/S0140-6736\(15\)00128-2](https://doi.org/10.1016/S0140-6736(15)00128-2)
- Frederickson, L.B., Russell, H.S., Fessa, D., Khan, J., Schmidt, J.A., Johnson, M.S., Hertel, O., 2023. Hyperlocal air pollution in an urban environment - measured with low-cost sensors. *Urban Clim* 52. <https://doi.org/10.1016/j.uclim.2023.101684>
- Frederickson, L.B., Sidaraviciute, R., Schmidt, J.A., Hertel, O., Johnson, M.S., 2022. Are dense networks of low-cost nodes better at monitoring air pollution? A case study in Staffordshire. *EGUsphere* 2022, 1–28.
- Fuller, R., Landrigan, P.J., Balakrishnan, K., Bathan, G., Bose-O'Reilly, S., Brauer, M., Caravanos, J., Chiles, T., Cohen, A., Corra, L., Cropper, M., Ferraro, G., Hanna, J., Hanrahan, D., Hu, H., Hunter, D., Janata, G., Kupka, R., Lanphear, B., Lichtveld, M., Martin, K., Mustapha, A., Sanchez-Triana, E., Sandilya, K., Schaeffli, L., Shaw, J., Seddon, J., Suk, W., Téllez-Rojo, M.M., Yan, C., 2022. Pollution and health: a progress update. *Lancet Planet Health* 6, e535–e547. [https://doi.org/10.1016/S2542-5196\(22\)00090-0](https://doi.org/10.1016/S2542-5196(22)00090-0)
- Giordano, M.R., Malings, C., Pandis, S.N., Presto, A.A., McNeill, V.F., Westervelt, D.M., Beekmann, M., Subramanian, R., 2021. From low-cost sensors to high-quality data: A summary of challenges and best practices for effectively calibrating low-cost particulate matter mass sensors. *J Aerosol Sci* 158, 105833. <https://doi.org/10.1016/j.jaerosci.2021.105833>

- Hagan, D., Kroll, J., 2020. Assessing the accuracy of low-cost optical particle sensors using a physics-based approach. *Atmospheric Measurement Techniques Discussions* 1–36. <https://doi.org/10.5194/amt-2020-188>
- Harrison, R.M., Beddows, D.C.S., Dall'Osto, M., 2011. PMF analysis of wide-range particle size spectra collected on a major highway. *Environ Sci Technol* 45, 5522–5528. <https://doi.org/10.1021/es2006622>
- Hassani, A., Castell, N., Watne, Å.K., Schneider, P., 2023. Citizen-operated mobile low-cost sensors for urban PM_{2.5} monitoring: field calibration, uncertainty estimation, and application. *Sustain Cities Soc* 95. <https://doi.org/10.1016/j.scs.2023.104607>
- Haugen, M., Singh, A., Bousiotis, D., Pope, F.D., Boies, A., 2022. Differentiating Semi-Volatile and Solid Particle Events Using Carbon Sensors. *Atmosphere (Basel)* 13.
- Hennig, F., Quass, U., Hellack, B., Küpper, M., Kuhlbusch, T.A.J., Stafoggia, M., Hoffmann, B., 2018. Ultrafine and fine particle number and surface area concentrations and daily cause-specific mortality in the Ruhr area, Germany, 2009–2014. *Environ Health Perspect* 126, 2009–2014. <https://doi.org/10.1289/EHP2054>
- Hong, J., Kang, H., Jung, S., Sung, S., Hong, T., Park, H.S., Lee, D.E., 2020. An empirical analysis of environmental pollutants on building construction sites for determining the real-time monitoring indices. *Build Environ* 170, 106636. <https://doi.org/10.1016/j.buildenv.2019.106636>
- Hopke, P.K., 2016. Review of receptor modeling methods for source apportionment. *J Air Waste Manage Assoc* 66, 237–259. <https://doi.org/10.1080/10962247.2016.1140693>
- Hopke, P.K., Dai, Q., Li, L., Feng, Y., 2020. Science of the Total Environment Global review of recent source apportionments for airborne particulate matter. *Science of the Total Environment* 740, 140091. <https://doi.org/10.1016/j.scitotenv.2020.140091>
- Ilyinskaya, E., Schmidt, A., Mather, T.A., Pope, F.D., Witham, C., Baxter, P., Jóhannsson, T., Pfeffer, M., Barsotti, S., Singh, A., Sanderson, P., Bergsson, B., McCormick Kilbride, B., Donovan, A., Peters, N., Oppenheimer, C., Edmonds, M., 2017. Understanding the environmental impacts of large fissure eruptions: Aerosol and gas emissions from the 2014–2015 Holuhraun eruption (Iceland). *Earth Planet Sci Lett* 472, 309–322. <https://doi.org/10.1016/j.epsl.2017.05.025>
- Kang, Y., Aye, L., Ngo, T.D., Zhou, J., 2022. Performance evaluation of low-cost air quality sensors: A review. *Science of the Total Environment*. <https://doi.org/10.1016/j.scitotenv.2021.151769>
- Karagulian, F., Barbieri, M., Kotsev, A., Spinelle, L., Gerboles, M., Lagler, F., Redon, N., Crunaire, S., Borowiak, A., 2019. Review of the performance of low-cost sensors for air quality monitoring. *Atmosphere (Basel)*. <https://doi.org/10.3390/atmos10090506>
- Karagulian, F., Belis, C.A., Francisco, C., Dora, C., Prüss-ustün, A.M., Bonjour, S., Adair-rohani, H., Amann, M., 2015. Contributions to cities' ambient particulate matter (PM): A systematic review of local source contributions at global level. *Atmos Environ* 120, 475–483. <https://doi.org/10.1016/j.atmosenv.2015.08.087>
- Khreis, H., Johnson, J., Jack, K., Dadashova, B., Park, E.S., 2022. Evaluating the Performance of Low-Cost Air Quality Monitors in Dallas, Texas.
- Kittelson, D., Watts, W., Johnson, J., 2003. Gasoline vehicle exhaust particle sampling study. *Proceedings of US ...* 1–11.
- Kortoçi, P., Hossein, N., Arbayani, M., Lun, P., Varjonen, S., Rebeiro-hargrave, A., Niemi, J. V., 2022. Air pollution exposure monitoring using portable low-cost air quality sensors 23. <https://doi.org/10.1016/j.smhl.2021.100241>

- Kumar, P., Morawska, L., Martani, C., Biskos, G., Neophytou, M., Di Sabatino, S., Bell, M., Norford, L., Britter, R., 2015. The rise of low-cost sensing for managing air pollution in cities. *Environ Int* 75, 199–205. <https://doi.org/10.1016/j.envint.2014.11.019>
- Lin, J.C., Fasoli, B., Mitchell, L., Bares, R., Hopkins, F., Thompson, T.M., Alvarez, R.A., 2023. Towards hyperlocal source identification of pollutants in cities by combining mobile measurements with atmospheric modeling. *Atmos Environ* 311. <https://doi.org/10.1016/j.atmosenv.2023.119995>
- Liu, C., Chen, R., Sera, F., Vicedo-Cabrera, A.M., Guo, Y., Tong, S., Coelho, M.S.Z.S., Saldiva, P.H.N., Lavigne, E., Matus, P., Valdes Ortega, N., Osorio Garcia, S., Pascal, M., Stafoggia, M., Scortichini, M., Hashizume, M., Honda, Y., Hurtado-Díaz, M., Cruz, J., Nunes, B., Teixeira, J.P., Kim, H., Tobias, A., Íñiguez, C., Forsberg, B., Åström, C., Ragettli, M.S., Guo, Y.-L., Chen, B.-Y., Bell, M.L., Wright, C.Y., Scovronick, N., Garland, R.M., Milojevic, A., Kyselý, J., Urban, A., Orru, H., Indermitte, E., Jaakkola, J.J.K., Rytí, N.R.I., Katsouyanni, K., Analitis, A., Zanobetti, A., Schwartz, J., Chen, J., Wu, T., Cohen, A., Gasparri, A., Kan, H., 2019. Ambient Particulate Air Pollution and Daily Mortality in 652 Cities. *New England Journal of Medicine* 381, 705–715. <https://doi.org/10.1056/nejmoa1817364>
- Lung, S.C., 2022. Arch̄ um Ateneo Research Priorities of Applying Low-Cost PM2.5 Sensors in Southeast Asian Countries.
- Macnaughton, P., Melly, S., Vallarino, J., Adamkiewicz, G., Spengler, J.D., 2014. Impact of bicycle route type on exposure to traffic-related air pollution. *Science of the Total Environment*, The 490, 37–43. <https://doi.org/10.1016/j.scitotenv.2014.04.111>
- Mills, S.A., Bousiotis, D., Maya-Manzano, J.M., Tummon, F., MacKenzie, A.R., Pope, F.D., 2023. Constructing a pollen proxy from low-cost Optical Particle Counter (OPC) data processed with Neural Networks and Random Forests. *Science of the Total Environment* 871, 161969. <https://doi.org/10.1016/j.scitotenv.2023.161969>
- Paatero, P., 2004. User guide for positive matrix factorisation programs PMF2 and PMF3, Part 1: tutorial. University of Helsinki, Helsinki, Finland.
- Paatero, P., Hopke, P.K., Song, X.H., Ramadan, Z., 2002. Understanding and controlling rotations in factor analytic models. *Chemometrics and Intelligent Laboratory Systems* 60, 253–264. [https://doi.org/10.1016/S0169-7439\(01\)00200-3](https://doi.org/10.1016/S0169-7439(01)00200-3)
- Paatero, P., Tapper, U., 1994. Positive Matrix Factorization : A Non-negative factor model with optimal utilization of error estimates of data values. *Environmetrics* 5, 111–126.
- Paatero, P., Tapper, U., 1993. Analysis of different modes of factor analysis as least squares fit problems. *Chemometrics and Intelligent Laboratory Systems* 18, 183–194. [https://doi.org/10.1016/0169-7439\(93\)80055-M](https://doi.org/10.1016/0169-7439(93)80055-M)
- Patel, S., Leavey, A., Sheshadri, A., Kumar, P., Kandikuppa, S., Tarsi, J., Mukhopadhyay, K., Johnson, P., Balakrishnan, K., Schechtman, K.B., Castro, M., Yadama, G., Biswas, P., 2018. Associations between household air pollution and reduced lung function in women and children in rural southern India. *Journal of Applied Toxicology* 38, 1405–1415. <https://doi.org/10.1002/jat.3659>
- Peltier, R.E., Núria Castell, A.L.C., Adrian Arfire, À.B., Peltier, R.E., 2021. An Update on Low-cost Sensors for the Measurement of Atmospheric Composition, December 2020, Wmo.
- Raysoni, A.U., Pinakana, S.D., Mendez, E., Wladyka, D., Sepielak, K., Temby, O., 2023. A Review of Literature on the Usage of Low-Cost Sensors to Measure Particulate Matter 168–186.

- Reff, A., Eberly, S.I., Bhawe, P. V., 2007. Receptor modeling of ambient particulate matter data using positive matrix factorization: Review of existing methods. *J Air Waste Manage Assoc* 57, 146–154. <https://doi.org/10.1080/10473289.2007.10465319>
- Rivas, I., Beddows, D.C.S., Amato, F., Green, D.C., Järvi, L., Hueglin, C., Reche, C., Timonen, H., Fuller, G.W., Niemi, J. V, Pérez, N., Aurela, M., Hopke, P.K., Alastuey, A., Kulmala, M., Harrison, R.M., Querol, X., Kelly, F.J., 2020. Source apportionment of particle number size distribution in urban background and traffic stations in four European cities. *Environ Int* 135, 105345. <https://doi.org/10.1016/j.envint.2019.105345>
- Rivas, I., Vicens, L., Basagaña, X., Tobías, A., Katsouyanni, K., Walton, H., Hüglin, C., Alastuey, A., Kulmala, M., Harrison, R.M., Pekkanen, J., Querol, X., Sunyer, J., Kelly, F.J., 2021. Associations between sources of particle number and mortality in four European cities. *Environ Int* 155. <https://doi.org/10.1016/j.envint.2021.106662>
- Robinson, J.A., Kocman, D., Horvat, M., Bartonova, A., 2018. End-user feedback on a low-cost portable air quality sensor system — Are we there yet? *Sensors (Switzerland)* 18, 20–22. <https://doi.org/10.3390/s18113768>
- Samad, A., Vogt, U., 2020. Urban Climate Investigation of urban air quality by performing mobile measurements using a bicycle (MOBAIR). *Urban Clim* 33, 100650. <https://doi.org/10.1016/j.uclim.2020.100650>
- Schmid, O., Stoeger, T., 2016. Surface area is the biologically most effective dose metric for acute nanoparticle toxicity in the lung. *J Aerosol Sci* 99, 133–143. <https://doi.org/10.1016/j.jaerosci.2015.12.006>
- Seakins, P.W., Lansley, D.L., Hodgson, A., Huntley, N., Pope, F.D., 2002. New Directions: Mobile laboratory reveals new issues in urban air quality. *Atmos Environ* 36, 1247–1248.
- Sekhavati, E., Yengejeh, R.J., 2023. Particulate matter exposure in construction sites is associated with health effects in workers. *Front Public Health* 11, 1130620. <https://doi.org/10.3389/fpubh.2023.1130620>
- Singh, A., Ng'ang'a, D., Gatari, M.J., Kidane, A.W., Alemu, Z.A., Derrick, N., Webster, M.J., Bartington, S.E., Thomas, G.N., Avis, W., Pope, F.D., 2021. Air quality assessment in three east african cities using calibrated low-cost sensors with a focus on road-based hotspots. *Environ Res Commun* 3. <https://doi.org/10.1088/2515-7620/ac0e0a>
- Solomon, P.A., Vallano, D., Lunden, M., Lafranchi, B., Blanchard, C.L., Shaw, S.L., 2020. Mobile-platform measurement of air pollutant concentrations in California : performance assessment , statistical methods for evaluating spatial variations , and spatial representativeness 3277–3301.
- Sousan, S., Koehler, K., Thomas, G., Park, J.H., Hillman, M., Halterman, A., Peters, T.M., 2016. Inter-comparison of low-cost sensors for measuring the mass concentration of occupational aerosols. *Aerosol Science and Technology* 50, 462–473. <https://doi.org/10.1080/02786826.2016.1162901>
- Wang, P., Xu, F., Gui, H., Wang, H., Chen, D.R., 2021. Effect of relative humidity on the performance of five cost-effective PM sensors. *Aerosol Science and Technology* 55, 957–974. <https://doi.org/10.1080/02786826.2021.1910136>
- Wang, S., Ma, Y., Wang, Z., Wang, L., Chi, X., Ding, A., Yao, M., Li, Y., 2021. Mobile monitoring of urban air quality at high spatial resolution by low-cost sensors : impacts of COVID-19 pandemic lockdown 7199–7215.
- Westervelt, D.M., Isevlambire, P.K., Yombo Phaka, R., Yang, L.H., Raheja, G., Milly, G., Selenge, J.-L.B., Mulumba, J.P.M., Bousiotis, D., Djibi, B.L., McNeill, V.F., Ng, N.L., Pope,

F., Mbela, G.K., Konde, J.N., 2023. Low-Cost Investigation into Sources of PM 2.5 in Kinshasa, Democratic Republic of the Congo . ACS ES&T Air.

<https://doi.org/10.1021/acsestair.3c00024>

World Health Organisation, 2021. WHO global air quality guidelines: particulate matter (PM2.5 and PM10), ozone, nitrogen dioxide, sulfur dioxide and carbon monoxide. World Health Organization, Geneva PP - Geneva.

ACKNOWLEDGMENTS

The materials and study were funded by the European Commission as part of the RI-URBANS project (grant no. 1010362450) and the UKRI (NE/T001968/1).

TABLE LEGENDS:

Table 1: Average conditions on each walk (row colour indicates the time of the day with Blue being morning, Black being afternoon and Brown being evening) measured by the LCS.

Table 2: Average PM_{10} , $PM_{2.5}$, PM_{10} , BC, PN and LDSA of the five factors.

Table 3: Average contribution of local and regional sources on the PM ($\mu\text{g m}^{-3}$), BC (ng m^{-3}), PN (N cm^{-3}) and LDSA ($\mu\text{m}^2 \text{cm}^{-3}$) concentrations.

FIGURE LEGENDS

Figure 1: Map of the study area (map ©Google). The construction signs refer to the construction sites in the area at the time of the campaign.

Figure 2: PolarAnnuli plots for the average concentrations PM_{10} , $PM_{2.5}$, PM_{10} and BC (a, b, c, d respectively) during the campaign measurement period, measured at the BAQS. The concentrations are calculated using the mean concentration of the observations for the different wind conditions and time of the day. Thus, the number of observations for each segment may differ.

Figure 3: Polar plots of the contribution of the factors. The position of each spot in the plot resembles the wind direction and speed (the further from the centre, the greater the wind speed) for which the measurements are averaged. The concentrations are calculated using the mean concentration of the observations for the different wind conditions and time of the day. Thus, the number of observations for each segment may differ.

Figure 4: Average G contribution (normalized to 1) per block for each factor (factor 1 to 5 is shown in figures (a) to (e) respectively) (each block is 0.001×0.001 longitude x latitude points, about $111\text{m} \times 111\text{m} = 12321 \text{m}^2$).

Figure 5: Average (a) $PM_{2.5}$ and (b) PM_{10} mass concentrations (in $\mu\text{g m}^{-3}$), (c) LDSA (in $\mu\text{m}^2 \text{cm}^{-3}$) and (d) Black carbon (in ng m^{-3}) concentrations during the walks of the campaign. The position of the points is the average position of the measurements per each block

Figure 6: Map of the road (a) and variation of the sources of $PM_{2.5}$ (b), PM_{10} (c) and LDSA (d) for a transect down Dawlish Road. The location of construction sites are highlighted on the PM_{10} figure.

Figure 7: Map of the road (a) and variation of the sources of $PM_{2.5}$ (b), PM_{10} (c) and LDSA (d) for a transect across Bristol Road. Major (on a junction) and minor (no junction) traffic light points are marked by symbols on the LDSA figure.

Day	PM ₁ ($\mu\text{g m}^{-3}$)	PM _{2.5} ($\mu\text{g m}^{-3}$)	PM ₁₀ ($\mu\text{g m}^{-3}$)	BC (ng m^{-3})	PN (N cm^{-3})	LDSA ($\mu\text{m}^2 \text{cm}^{-3}$)	WD (deg)	WS (m s^{-1})
Thursday 15/6	3.07	7.07	29.5	2733	15812	25.4	NE	1.68
Friday 16/6	2.50	5.59	26.3	2424	18592	26.4	E	1.72
Sunday 18/6	6.68	9.87	22.6	2450	14935	24.3	E	1.56
Monday 19/6	3.91	8.77	20.0	1938	15346	13.8	SW	2.46
Monday 19/6	2.60	6.42	20.7	1615	16877	18.6	SW	1.89
Tuesday 20/6	2.23	4.55	15.1	1953	16513	18.7	SW	0.92
Thursday 22/6	4.49	8.05	22.6	2688	22195	27.4	Mixed	1.04
Sunday 25/6	3.17	5.88	21.8	2173	13211	24.2	SW	2.76
Sunday 25/6	1.75	5.03	20.3	1047	10108	13.3	SW	1.53
Monday 26/6	1.28	3.97	16.6	1309	16143	11.7	SW	1.91

Table 1: Average conditions on each walk (row colour indicates the time of the day with Blue being morning, Black being afternoon and Brown being evening) measured by the LCS.

	PM ₁ ($\mu\text{g m}^{-3}$)	PM _{2.5} ($\mu\text{g m}^{-3}$)	PM ₁₀ ($\mu\text{g m}^{-3}$)	BC (ng m^{-3})	PN (N cm^{-3})	LDSA ($\mu\text{m}^2 \text{cm}^{-3}$)
F1 (Urban background)	1.58	2.21	1.24	614	Negligible	3.29
F2 (Local)	0.02	0.13	2.32	Negligible	Negligible	0.10
F3 (Marine)	0.79	3.22	3.90	Negligible	2460	Negligible
F4 (Local)	0.08	1.01	5.36	20	Negligible	0.80
F5 (Traffic)	0.07	0.17	0.76	676	11388	13.5
Unexplained	0.16	0.43	3.36	696	2124	2.34

Table 2: Average PM₁, PM_{2.5}, PM₁₀, BC, PN and LDSA of the five factors

	Local sources contribution	Regional sources contribution	Local sources %	Regional sources %
PM ₁	0.2	2.4	6.6	93.4
PM _{2.5}	1.3	5.4	19.4	80.6
PM ₁₀	8.4	5.2	62.2	37.8
BC	696	614	53.1	46.9
PN	11388	2460	82.2	17.8
LDSA	14.4	3.3	81.4	18.6

Table 3: Average contribution of local and regional sources on the PM ($\mu\text{g m}^{-3}$), BC (ng m^{-3}), PN (N cm^{-3}) and LDSA ($\mu\text{m}^2 \text{cm}^{-3}$) concentrations



Figure 1: Map of the study area (map ©Google). The construction signs refer to the construction sites in the area at the time of the campaign.

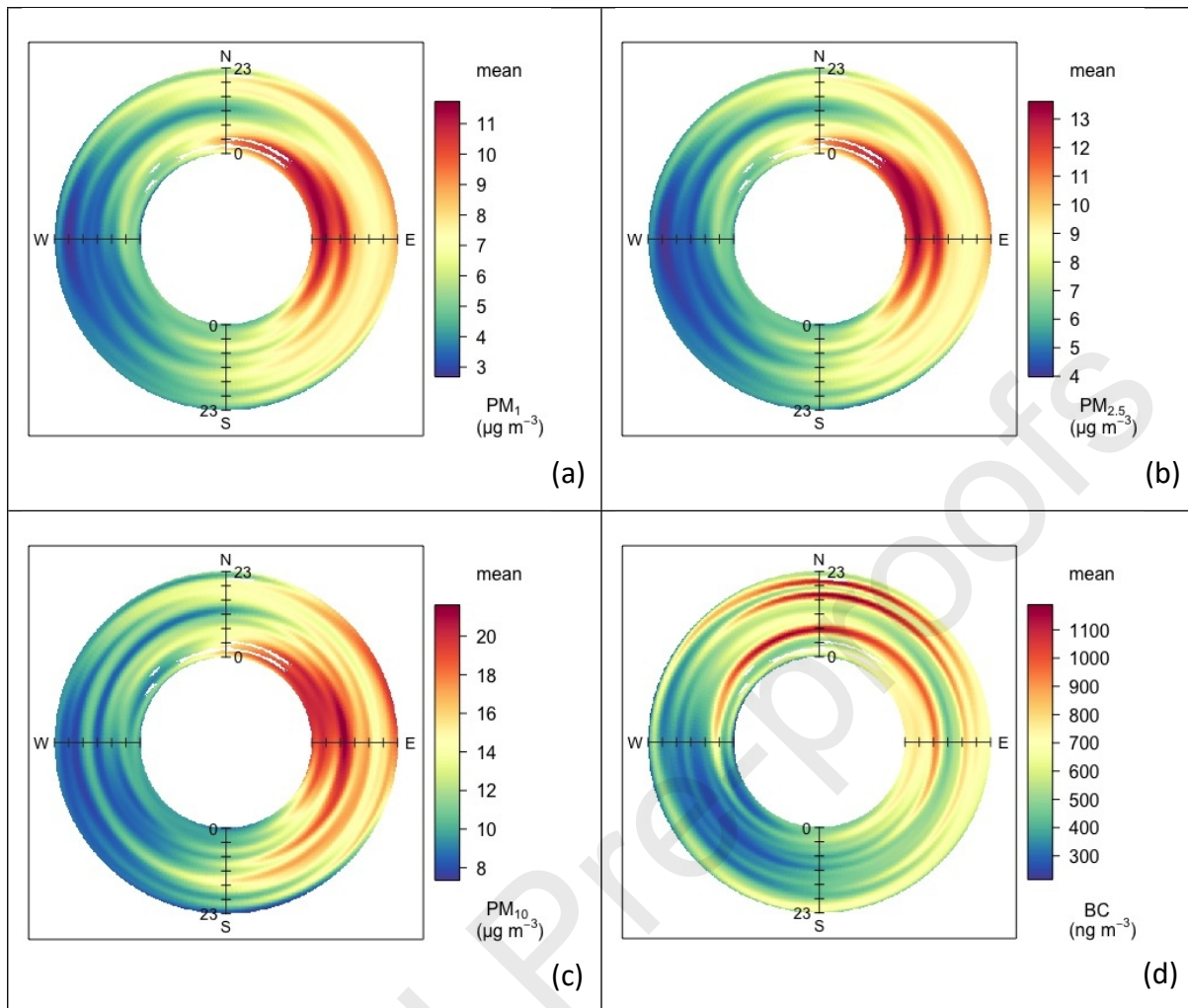


Figure 2: PolarAnnuli plots for the average concentrations PM_{1} , $PM_{2.5}$, PM_{10} and BC (a, b, c, d respectively) during the campaign measurement period, measured at the BAQS. The concentrations are calculated using the mean concentration of the observations for the different wind conditions and time of the day. Thus, the number of observations for each segment may differ.

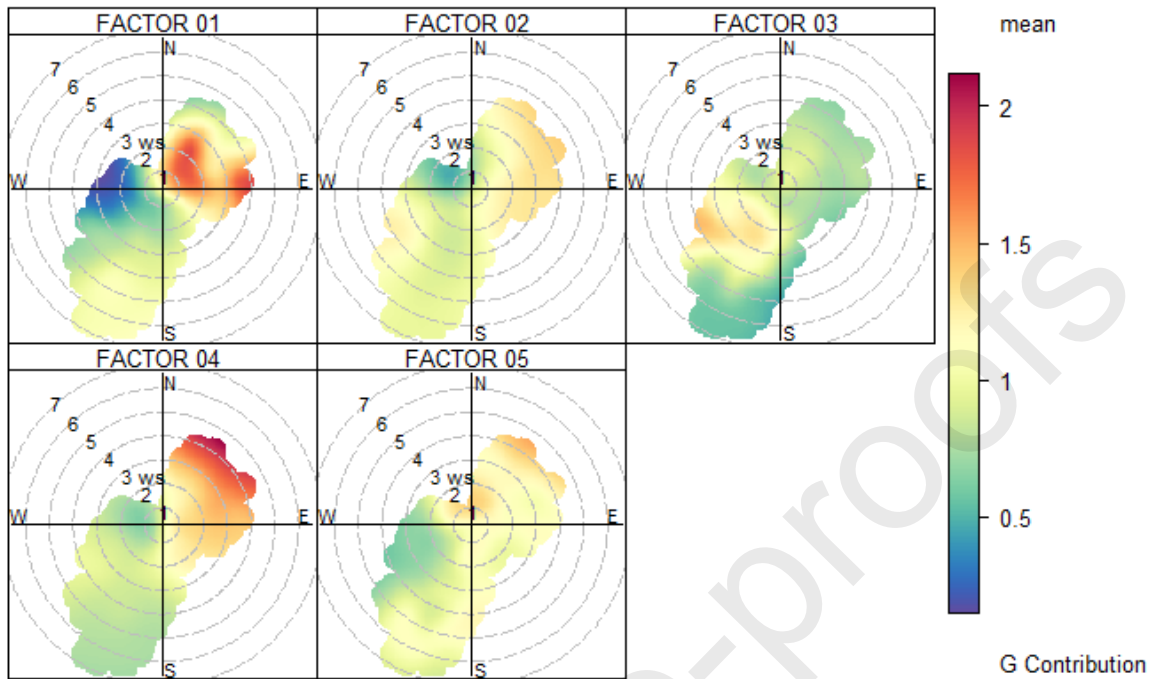


Figure 3: Polar plots of the contribution of the factors. The position of each spot in the plot resembles the wind direction and speed (the further from the centre, the greater the wind speed) for which the measurements are averaged. The concentrations are calculated using the mean concentration of the observations for the different wind conditions and time of the day. Thus, the number of observations for each segment may differ.

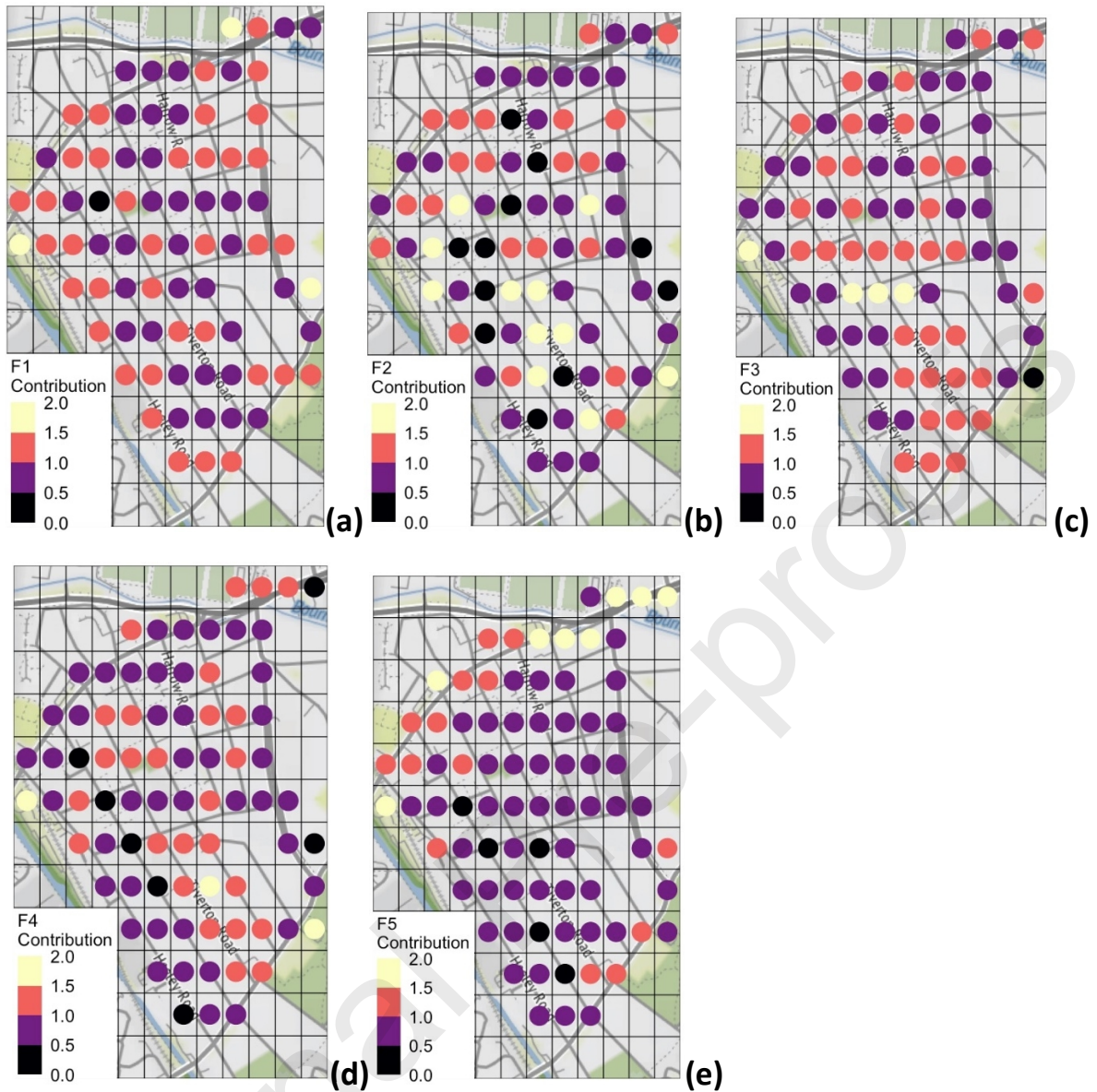


Figure 4: Average G contribution (normalized to 1) per block for each factor (factor 1 to 5 is shown in figures (a) to (e) respectively) (each block is 0.001×0.001 longitude x latitude points, about $111m \times 111m = 12321 m^2$).

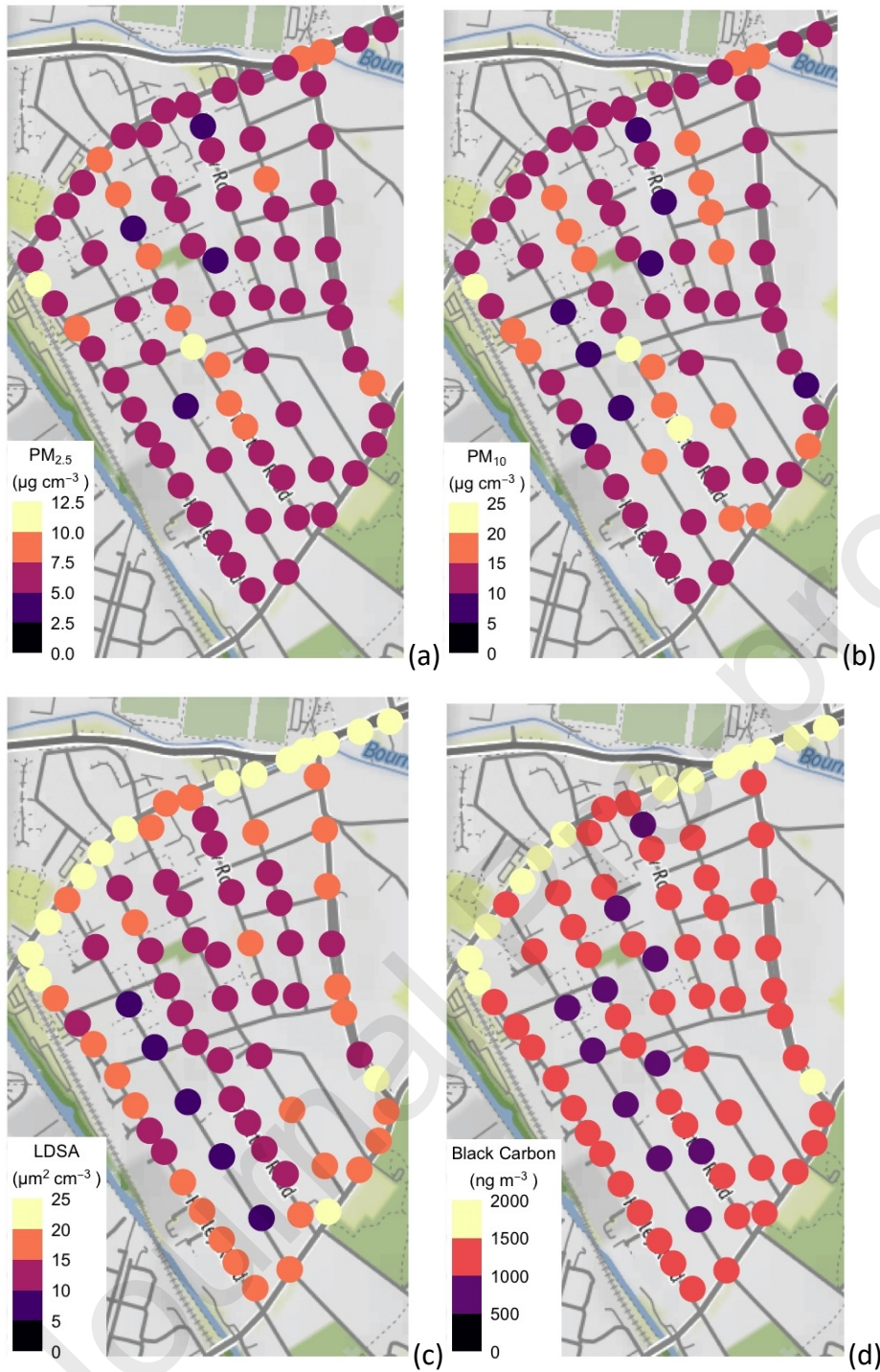


Figure 5: Average (a) $PM_{2.5}$ and (b) PM_{10} mass concentrations (in $\mu g\ m^{-3}$), (c) LDSA (in $\mu m^2\ cm^{-3}$) and (d) Black carbon (in $ng\ m^{-3}$) concentrations during the walks of the campaign. The position of the points is the average position of the measurements per each block.

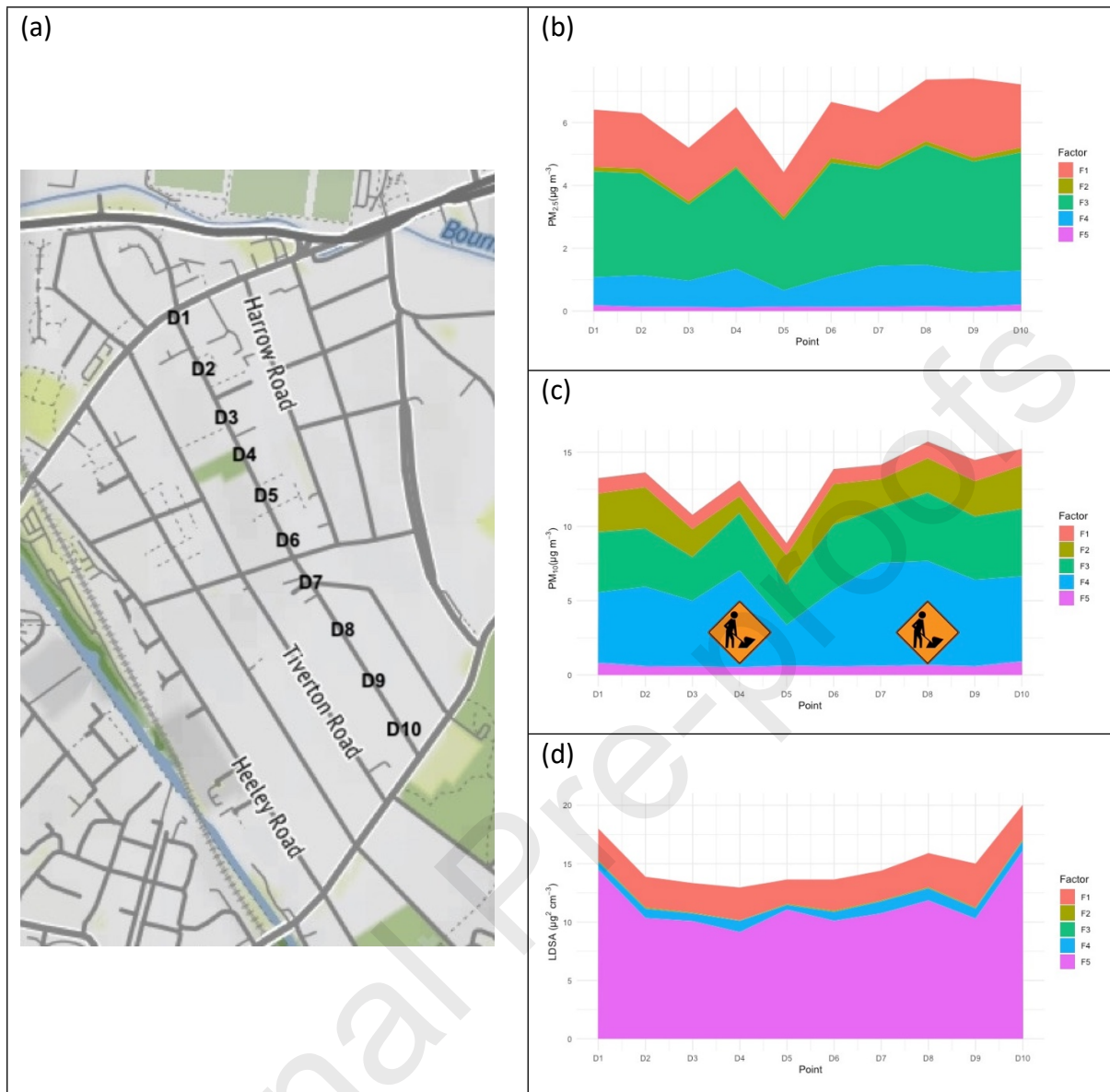


Figure 6: Map of the road (a) and variation of the sources of $PM_{2.5}$ (b), PM_{10} (c) and LDSA (d) for a transect down Dawlish Road. The location of construction sites are highlighted on the PM_{10} figure.

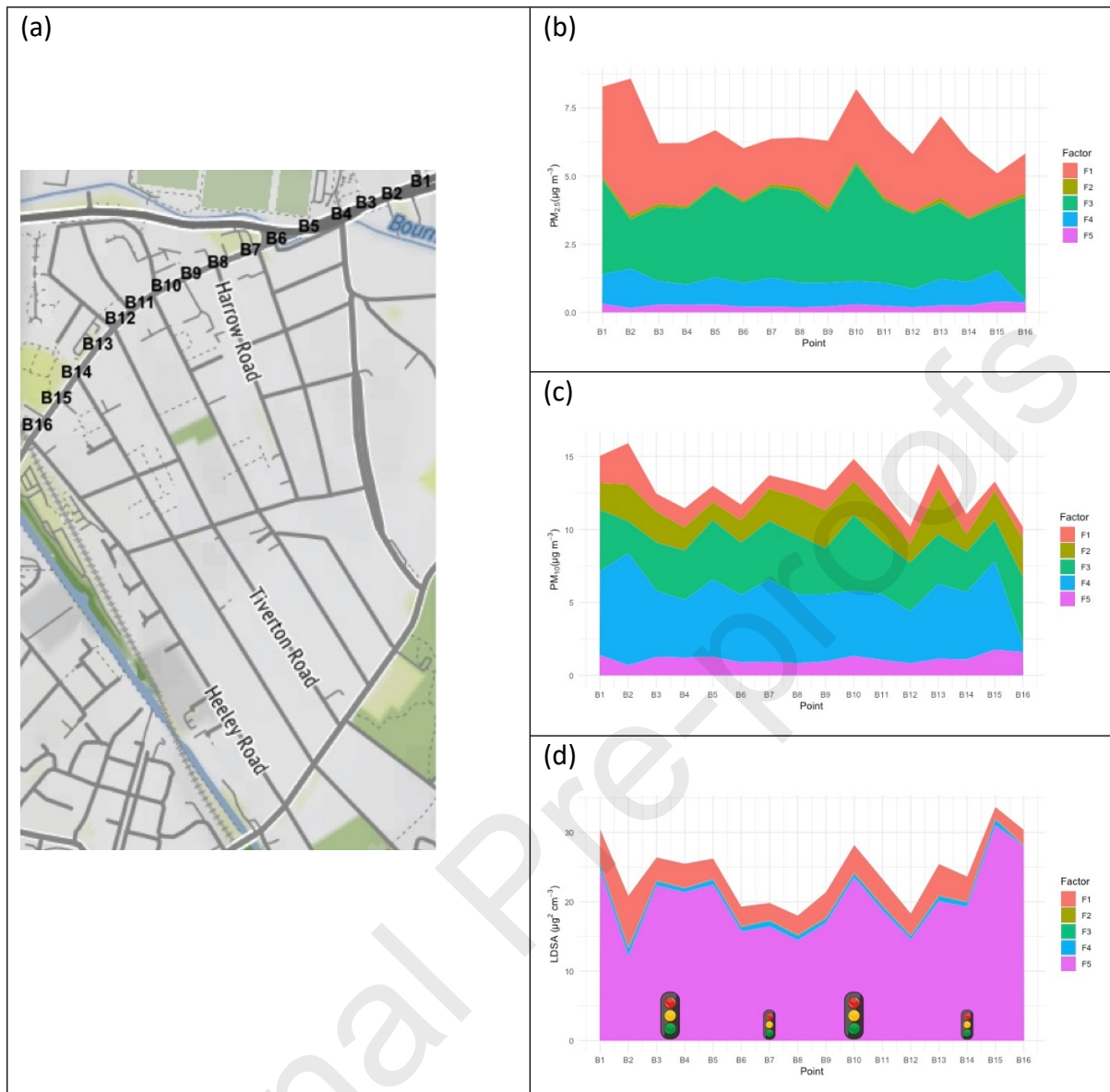


Figure 7. Map of the road (a) and variation of the sources of PM_{2.5} (b), PM₁₀ (c) and LDSA (d) for a transect across Bristol Road. Major (on a junction) and minor (no junction) traffic light points are marked by symbols on the LDSA figure.

Declaration of interests

The authors declare that they have no known competing financial interests or personal relationships that could have appeared to influence the work reported in this paper.

The authors declare the following financial interests/personal relationships which may be considered as potential competing interests:

CRedit author statement

Dimitrios Bousiotis: Conceptualization, Methodology, Validation, Formal analysis, Data curation, Writing – Original draft, Visualization, Project administration

Seny Damayanti: Investigation, Writing – Review & Editing

Arunik Baruah: Investigation, Writing – Review & Editing

Alessandro Bigi: Writing – Review & Editing

David C.S. Beddows: Methodology, Software, Writing – Review & Editing

Roy M. Harrison: Writing – Review & Editing, Funding acquisition

Francis D. Pope: Conceptualization, Writing – Review & Editing, Supervision, Project administration, Funding acquisition